

Radiation and Climate

**From Radiative Transfer Modelling
to Global Temperature Response**

Rob van Dorland

Keywords: radiation, atmospheric composition, greenhouse effect, climate

Printed by Ponsen & Looijen, Wageningen

ISBN 90-646-4032-7

Cover page: Geographical distribution of the January (front page) and July (back page) mean total anthropogenic radiative forcing between 1850-1990 due to changes of well-mixed greenhouse gases (CO₂, CH₄, N₂O, and CFCs), tropospheric ozone and sulfate aerosols (direct effect) as calculated by the radiative transfer model (coloured shading). Observed global and annual mean temperature since 1856 (source: *Jones*, 1994 and updated until 1998) (solid black curve).

Radiation and Climate

From Radiative Transfer Modelling to Global Temperature Response

Straling en Klimaat

Van Stralingstransportberekeningen tot Mondiale Temperatuurrepons

(met een samenvatting in het Nederlands)

Proefschrift ter verkrijging van de graad van doctor aan de Universiteit Utrecht op gezag van de Rector Magnificus, Prof. Dr. H.O. Voorma ingevolge het besluit van het College voor Promoties in het openbaar te verdedigen op maandag 15 november 1999 des middags te 16.15 uur

door

Rob van Dorland

geboren op 17 januari 1959, te Utrecht

Promotor: Prof. Dr. A.A.M. Holtslag
Faculteit Natuur- en Sterrenkunde, Universiteit Utrecht
en Meteorologie en Luchtkwaliteit, Wageningen Universiteit

Co-promotor: Dr. P. Stammes
Koninklijk Nederlands Meteorologisch Instituut

Dit onderzoek werd mogelijk gemaakt door het Koninklijk Nederlands Meteorologisch Instituut (KNMI)

The research described in this thesis was performed and supported by the Royal Netherlands Meteorological Institute (KNMI)

Contents

Voorwoord	ix
Samenvatting	xiii
1 General Introduction	1
1.1 Motivation	1
1.2 Outline of the Thesis	3
1.2.1 Radiation, Greenhouse Effect and Climate Change	3
1.2.2 Radiative Transfer Scheme	3
1.2.3 Climate Studies	4
2 Atmospheric Radiative Transfer, Greenhouse Effect and Climate Change	7
2.1 Introduction	7
2.2 Historical Perceptions of the Greenhouse Effect	9
2.2.1 Concepts in the Nineteenth Century	9
2.2.2 Developments in the Twentieth Century	10
2.3 Interaction between Matter and Radiation	11
2.3.1 Terminology	11
2.3.2 Black Body Radiation	13
2.3.3 Radiative Transfer Equation	15
2.4 Global Energy Balance and Radiative Forcing	16
2.4.1 Global Energy Balance	16
2.4.2 Concept of Radiative Forcing	20
2.4.3 Climate Effects of Atmospheric Constituents	21
2.5 Analysis of the greenhouse effect	23
2.5.1 Simple Analytical Model for Longwave Radiative Transfer Characteristics	23
2.5.2 Enhanced Greenhouse Effect	27
2.5.3 Analysis in Terms of Effective Temperature	31
2.6 The Science of Climate Change	34
2.6.1 Climate Issues	34
2.6.2 Climate Change	35
2.6.3 Climate Models	37
2.6.4 Uncertainties in Climate Response	38
2.7 Summary and Conclusions	38

3	A Longwave Radiative Transfer Scheme for Climate Modelling and its Evaluation with Surface Observations at Cabauw	43
3.1	Introduction	44
3.2	Theory and Background	45
3.2.1	Longwave Radiative Transfer	45
3.2.2	Description of the Narrow Band Scheme	46
3.2.3	Spectroscopic Datasets	47
3.3	Experiments with the Narrow Band Scheme	50
3.4	The Wide Band Radiation Scheme	55
3.4.1	Transmissivity Parameterizations	55
3.4.2	Comparison with the Narrow Band Scheme	57
3.5	Evaluation of the Wide Band Scheme at the Surface	57
3.5.1	Cabauw Observations and Data Quality	57
3.5.2	Model Inputs and Sensitivity	60
3.5.3	Comparison of the Wide Band Scheme with Observations	61
3.6	Summary and Conclusions	62
3.A	Appendix: Processing Spectroscopic Line Parameters	66
3.A.1	Temperature and Pressure Dependencies	66
3.A.2	Random Band Models	66
4	Radiative Forcing due to Tropospheric Ozone and Sulfate Aerosols	69
4.1	Introduction	70
4.2	Model Description	72
4.2.1	Concept of Radiative Forcing	72
4.2.2	Radiation Model	72
4.2.3	Input Data	73
4.2.4	Radiative Boundary Conditions	74
4.3	Radiative Forcing due to Tropospheric Ozone Changes	74
4.3.1	Ozone Changes 1850-1990	74
4.3.2	Ozone Changes 1990-2050	76
4.3.3	Ozone Radiative Forcing Sensitivity	77
4.3.4	Comparison of Results With Previous Work	80
4.4	Radiative Forcing due to Tropospheric Sulfate Changes	82
4.4.1	Optical Parameters	82
4.4.2	Sulfate Aerosol Changes 1850-1990	83
4.4.3	Nitrate Aerosol Changes 1850-1990	87
4.4.4	Sulfate Aerosol Changes 1990-2050	87
4.4.5	Sulfate Aerosol Radiative Forcing Sensitivity	89

Contents

4.4.6	Comparison of Results With Previous Work	89
4.5	Analytical Fits for Ozone and Sulfate Shortwave Forcing	90
4.5.1	Ozone	91
4.5.2	Sulfate Aerosols	92
4.6	Discussion	95
4.6.1	Ozone and Sulfate	95
4.6.2	Changes of the Radiation Balance for 1850-1990	100
4.7	Conclusion	100
5	Natural and Anthropogenic Variations in the Radiation Balance	105
5.1	Introduction	105
5.2	Radiation and Climate	107
5.3	Model Description	109
5.3.1	Radiative-Convective Model	109
5.3.2	Model Characteristics	110
5.3.3	Model Input	112
5.4	Model Results	114
5.4.1	Climate Response	114
5.4.2	Uncertainties in Climate Response	114
5.4.3	Statistical Optimization of Temperature Signals	117
5.5	Discussion and Conclusion	120
6	Summary and Outlook	125
6.1	Summary	125
6.2	Outlook	129
	References	133
	List of Acronyms and Abbreviations	143
	List of Publications	145
	Curriculum Vitae	147

¹R. van Dorland, P. Stammes, A.A.M. Holtslag, and W. Kohsiek, A longwave radiative transfer scheme for climate modelling and its evaluation with surface measurements at Cabauw, submitted to *Quart. J. Roy. Met. Soc.*, 1999.

²R. van Dorland, F.J. Dentener, and J. Lelieveld, *J. Geophys. Res.*, *102*, 28,079-28,100, 1997.

³R. van Dorland, and A.P. van Ulden, Natural and anthropogenic variations in the radiation balance, in *proceedings Sun and Climate: the influence of variations in solar activity on the earth's climate*, 1998.

Voorwoord

Het thema broeikasewfect en klimaatverandering is een veelbesproken onderwerp in de media. Niet alleen zijn er regelmatig meldingen van interessante ontwikkelingen binnen dit inmiddels multidisciplinaire vakgebied, ook levert ongelooft bij critici over de invloed van de mens op het klimaat een goede voedingsbodem voor de stroom aan berichten. Bovendien ligt het onderwerp politiek gevoelig: enerzijds bevinden we ons in een tijd waarin de omvang van het versterkte broeikasewfect nog in hoge mate onzeker is. Anderzijds is er sprake van een reëel risico van allerlei klimaateffecten, die tevens langdurig zullen zijn vanwege de verblijftijden van de belangrijkste broeikasgassen in de atmosfeer. Dit betekent dat nu wereldwijd emissiebeperkende maatregelen moeten worden overwogen, waaraan uiteraard kosten verbonden zijn. De maatschappelijke relevantie van het klimaatonderzoek is voor mij zeker een belangrijke drijfveer geweest.

Ook de Nederlandse overheid heeft het belang van klimaatonderzoek onderkend. Eind jaren tachtig heeft dit geleid tot het opzetten van een onderzoeksgroep op het KNMI en werd klimaatonderzoek één van de kerntaken van dit instituut. Binnen deze groep ben ik sinds 1988 werkzaam, hoewel de organisatiestructuur in de jaren daarna drastisch gewijzigd is. Veel dank ben ik verschuldigd aan Fons Baede, in die tijd hoofd van de afdeling Dynamische Meteorologie, Arie Kattenberg, trekker van het klimaatonderzoek en werkzaam bij de afdeling Oceanografisch Onderzoek, en mijn directe collega's, Rein Haarsma en Peter Siegmund. Al gauw werd duidelijk dat ik me zou toeleggen op atmosferisch stralingstransport in relatie met het broeikasewfect. Na een literatuurstudie over dit onderwerp, ben ik op werkbezoek geweest bij Jean-Jacques Morcrette (ECMWF), die als deskundige mij wegwijst heeft gemaakt in de stralingsprogrammatuur van het ECMWF. Zijn stralingstransportmodellen vormden het basisgereedschap van mijn onderzoek. Voor klimaattoepassingen is dit schema uitgebreid met allerlei broeikasgassen en aerosolen. Al snel had het Max Planck Institut für Meteorologie (Hamburg, Duitsland) belangstelling om het door mij te wijzigen stralingsmodel in te bouwen in het ECHAM klimaatmodel. Er ontstond een vruchtbare samenwerking met dit instituut, waarvoor ik in ieder geval Erich Roeckner en Ulrich Schlese wil bedanken.

In 1992 werd deze samenwerking verder vormgegeven door deelname aan het Europese project SINDICATE (Study of INdirect and DIrect Climate influences of Anthropogenic Trace gas Emissions). Binnen dit samenwerkingsverband heb ik veel opgestoken van chemische processen in de atmosfeer en in het algemeen van het bouwen en afregelen van complexe klimaatmodellen. De vele discussies zijn voor mij zeer waardevol geweest. In het bijzonder wil ik hiervoor Lennart Bengtsson, Paul Crutzen en Henning Rodhe bedanken. Via dit project ontstond ook binnen het KNMI een vruchtbare samenwerking met Hennie Kelder: Paul Fortuin werd op projectbasis aangehouden en met hem heb ik gedurende enkele jaren studies gedaan naar de stralingsforcering voornamelijk ten gevolge van ozonveranderingen. Eveneens is via SINDICATE een samenwerking

ontstaan met Jos Lelieveld, Frank Dentener en Geert-Jan Roelofs, nu verbonden aan het IMAU. Dit mondde uit in verscheidene publicaties, waarvan er één is opgenomen in dit proefschrift. Voorts heeft het mij verheugd om onderzoekers, zowel binnen als buiten het KNMI, mijn expertise op het gebied van stralingstransport desgevraagd aan te bieden. Hierbij wil ik in ieder geval de prettige samenwerking noemen met Jules Beersma, Michiel Schaeffer en Frank Selten onder auspiciën van Theo Opsteegh met betrekking tot het inbouwen van een vereenvoudigde versie van het stralingsschema in het ECBILT model.

Een grote stimulans bij het doen van onderzoek naar het versterkte broeikas-effect is voor mij de publieke belangstelling voor dit onderwerp geweest. Vanaf het begin heb ik publieksvoorlichting als één van mijn taken gezien. Niet alleen het geven van lezingen en interviews, maar zeker ook het schrijven van populair wetenschappelijke verhalen over diverse aspecten van het klimaatonderzoek hebben mij altijd veel voldoening gegeven. Hieraan heeft de gehele redactie van het maandblad *Zenit*, waarin ik de meteorologie voor mijn rekening neem, positief aan bijgedragen, waarvoor mijn dank.

Als hoogtepunten in mijn werk beschouw ik het broeikasdebat met dr. Jack Barrett (UK) over de stralingseffecten van CO₂ in september 1995 en mijn participatie in het symposium over de mogelijke invloed van variaties in zonne-activiteit op het klimaat in november 1997. Het onderzoek naar de klimaatinvloed van de zon heb ik samen met Aad van Ulden uitgevoerd en is opgenomen in dit proefschrift. Beide discussies ontstonden naar aanleiding van publicaties waarin de menselijke invloed op het klimaat in twijfel werd getrokken en de berichtgeving daarover in de landelijke pers. Aangezien omgaan met de media andere vaardigheden vereist dan het doen van onderzoek, ben ik Harry Geurts zeer erkentelijk voor zijn hulp en adviezen.

Een speciaal woord van dank wil ik besteden aan gepensioneerd KNMI'er Wouter Lablans. Zijn regelmatige gang naar mijn kamer en de vele gezamenlijke lunches met als doel een goed gesprek over een scala van (meteorologische) onderwerpen, hebben voor mij veel betekend. Zonder zijn kritische opmerkingen, tekstueel maar vooral ook inhoudelijk, zou dit proefschrift en in het bijzonder hoofdstuk 2 er anders uit gezien hebben. Zo bleek de 'Lablanstest' van de door mij geproduceerde teksten iedere keer weer essentieel.

Ook wil ik mijn kamergenoten, in chronologische volgorde Marc Allaart, Liu Qing, Nicole van Lipzig, Harry Carolus en Dave Donovan, bedanken voor hun gezelligheid en boeiende gesprekken. Marc heeft mij in de eerste jaren op het KNMI wegwijs gemaakt in de computersystemen van zowel het KNMI als het ECMWF. Nicole met wie ik de laatste vijf jaar de kamer heb gedeeld, wil ik ook bedanken voor haar hulp. Zonder haar had het mij aanzienlijk meer tijd gekost om de layout van dit proefschrift goed te krijgen. Mijn collega's op het KNMI wil ik bedanken voor hun belangstelling en de discussies, die mijns inziens essentieel zijn voor het uitvoeren van wetenschappelijk onderzoek.

Tenslotte beland ik bij mijn co-promotor, Piet Stammes, en promotor, Bert Holtslag. Aan hen heb ik veel te danken. Niet alleen zagen zij brood in mijn onderzoek, ook hebben zij veel werk verricht om mijn teksten te corrigeren en te structureren. Tevens is het ons gelukt om

Voorwoord

een gezamenlijke publikatie (met Wim Kohsiek als derde co-auteur) te schrijven. In tijden van tegenslag zijn zij onmisbaar gebleken.

En dan mijn vrouw, Jacqueline, en kinderen, Kim, Niels en Esther, die vaak veel geduld moesten opbrengen als ik weer eens een zaterdag of zondag (en soms beide dagen) nodig had om op het KNMI 'bij te werken'. Hun steun was essentieel voor de totstand koming van dit proefschrift!

Samenvatting

De versterking van het broeikaseffect ten gevolge van de uitstoot van broeikasgassen, in het bijzonder kooldioxide (CO_2), geniet al geruime tijd de belangstelling van de wetenschap en de politiek: klimaatonderzoek is niet alleen een boeiend vakgebied, maar er staan ook grote belangen op het spel. Enerzijds bestaat het risico van een gestage wereldwijde klimaatverandering, namelijk een toename van de gemiddelde temperatuur nabij het aardoppervlak in een tijdsbestek van honderd jaar, die qua orde van grootte vergelijkbaar is met het verschil in gemiddelde temperatuur tussen de laatste ijstijd en nu. Anderzijds vergt het reduceren van de broeikasgasemissies een grote inspanning van de mensheid. De lasten, die het terugdringen van de versterking van het broeikaseffect op korte termijn met zich meebrengt, geven aanleiding tot de vraag of de wetenschap het wel bij het rechte eind heeft. Met andere woorden: is de mens eigenlijk wel in staat om het klimaat ingrijpend te veranderen? Hoewel onze kennis van het klimaatsysteem verre van compleet is, mag de complexiteit van het probleem geen argument zijn om onbezorgd de mogelijke menselijke beïnvloeding van het klimaat af te wachten. De huidige onderzoekspanningen zijn gericht op het beter begrijpen van het klimaatsysteem in al haar details en het verkleinen van de bestaande onzekerheidsmarges.

In dit proefschrift, getiteld 'straling en klimaat (van stralingstransportberekeningen tot mondiale temperatuurrepons)', leggen we ons toe op atmosferische straling en de veranderingen daarin gedurende de laatste anderhalve eeuw. Gedurende deze periode is de samenstelling van de atmosfeer drastisch veranderd door menselijke activiteiten. Zo is de CO_2 concentratie met ruim 30% gestegen, terwijl ook broeikasgassen, zoals methaan (CH_4), lachgas (N_2O), en chloorfluorkoolstoffen (CFKs) een toename laten zien. Bovendien leidt de uitstoot van stikstof- en zwavelhoudende gassen via chemische reacties tot de vorming van het broeikasgas ozon en aërosolen. Deze sulfaat- en nitraataërosolen hebben een koelend effect op het klimaat, waarmee ze het versterkte broeikaseffect gedeeltelijk compenseren.

Om de effecten van bovengenoemde veranderingen te bestuderen wordt in dit proefschrift gebruik gemaakt van een stralingsschema, d.w.z. een computerprogramma waarmee atmosferisch stralingstransport berekend kan worden. Dit schema omvat de stralingseigenschappen van alle broeikasgassen en aërosolen, die van belang zijn voor klimaatstudies. Het stralingsschema wordt geëvalueerd met metingen van de neergaande langgolvlige straling aan het aardoppervlak. Voorts wordt een één-dimensionaal gekoppeld atmosfeer-oceaanmodel (klimaatmodel) ontwikkeld, waarin het stralingsschema een centrale rol inneemt. Het stralingsmodel en het klimaatmodel worden gebruikt om respectievelijk de stralingsforcering en de daarop volgende temperatuurrepons voor allerlei antropogene en natuurlijke forceringsmechanismen te berekenen.

We hebben voor deze benadering gekozen, omdat verstoringen van de stralingsbalans sterk

gekoppeld zijn aan de uiteindelijke temperatuurveranderingen nabij het aardoppervlak, althans op mondiale schaal. Als maat voor de verstoring van de stralingsbalans wordt de verandering van de netto stralingsflux ter hoogte van de tropopauze genomen. De gemiddelde tropopauze hoogte is zo'n 13 km. Deze fluxverandering, uitgedrukt in Wm^{-2} , wordt ook wel stralingsforcering genoemd. Bij de vertaalslag van stralingsforcering naar uiteindelijke temperatuurverandering zijn de temperatuurafhankelijke fysische processen in het klimaatsysteem van belang, omdat zij terugkoppelen naar temperatuurveranderingen. Deze omrekeningsfactor wordt ook wel klimaatgevoeligheid genoemd en wordt uitgedrukt in K per Wm^{-2} . Hoe groter de gevoeligheid, des te sterker is de temperatuurverandering voor een zekere stralingsforcering. De sterkte van de klimaatgevoeligheid is in hoge mate onzeker, maar wel voor alle forceringsmechanismen gelijk, omdat zij voornamelijk afhangt van de terugkoppelingen. Daarom kan een relatieve schatting gemaakt worden van klimaateffecten door bestudering van stralingsforceringen. Bovendien rechtvaardigt dit het gebruik van één-dimensionale gekoppelde atmosfeer-oceaanmodellen om het verloop van de klimaateffecten in de tijd ten gevolge van geleidelijke verandering in de samenstelling van de atmosfeer of andere oorzaken te bestuderen.

In hoofdstuk 2 wordt bovengenoemde aanpak uitgebreid toegelicht. Dit hoofdstuk kan dan ook beschouwd worden als grondige introductie op het thema straling en klimaat. We beginnen hier met een beknopte historische beschrijving van de denkbeelden van het versterkte broeikaseffect in de laatste twee eeuwen. Voorts worden de terminologie en basisprincipes van de wisselwerking tussen straling en materie, toegepast op atmosferisch stralingstransport, besproken. We besteden aandacht aan de mondiaal gemiddelde energiebalans. Met behulp van het één-dimensionale klimaatmodel berekenen we de bijdragen van de belangrijkste broeikasgassen aan de energiebalans. De aanwezigheid en verticale verdeling van deze gassen leiden tot een typische temperatuurstructuur van de wereldgemiddelde atmosfeer. Deze structuur is niet alleen van belang voor het langgolvig stralingstransport, maar ook voor het verband tussen stralingsforcering en uiteindelijke klimaateffect. We vereenvoudigen de langgolvige stralingstransportvergelijking tot een analytisch model voor de troposfeer (onderste 13 km van de atmosfeer) met slechts drie parameters. Hiermee kunnen de stralingsfluxen kwalitatief goed beschreven worden, hetgeen aangetoond wordt door vergelijking met nauwkeurige stralingsberekeningen. De gemiddelde weglengte tussen geëmitteerde en geabsorbeerde langgolvige straling is sterk afhankelijk van de beschouwde golflengte en is daarom een belangrijke parameter in onze analyse. Met dit analytische model kan het mechanisme van het versterkte broeikaseffect zowel in het transparante gedeelte van het spectrum, het zogeheten atmosferisch venster, als daarbuiten bestudeerd worden. Een verkeerde interpretatie van dit mechanisme is in het verleden regelmatig aanleiding geweest tot het in twijfel trekken van de menselijke invloed op het klimaat [Barrett, 1995; en bediscussieerd door Van Dorland, 1995]. Voorts wordt in dit hoofdstuk op het gevolg van verstoringen van de stralingsbalans ingegaan, namelijk mondiale klimaatverandering.

Achtereenvolgens wordt een overzicht gegeven van de centrale vraagstelling in het klimaatonderzoek, de potentiële oorzaken van klimaatverandering, de klimaatmodellen, en de oorzaken van onzekerheid voor de menselijke invloed. De belangrijkste conclusies van hoofdstuk 2 zijn:

- Een toename van broeikasgassen in de wereldgemiddelde atmosfeer leidt instantaan altijd tot een reductie van de opwaartse langgolvlige straling en een toename van de neerwaartse component op tropopauze hoogte. De reductie van de opwaartse flux hangt direct samen met de gemiddelde afname van de temperatuur met de hoogte. Voor gassen actief in het atmosferisch venster, zoals CFK's, wordt deze reductie veroorzaakt door de toename van absorptie van straling afkomstig van het aardoppervlak. Voor gassen actief buiten het atmosferisch venster, zoals het geval is voor de belangrijkste absorptiebanden van CO₂, is de verandering van straling afkomstig van de atmosfeer zelf van belang. Deze verandering wordt veroorzaakt door een toename van zowel absorptie als emissie van atmosferische straling.

- Verzadiging treedt op in een smal spectraal gebied, circa 0.05 μm breed, in het centrum van de 15 μm CO₂ band. Vanwege de sterkte van deze band in combinatie met de huidige dichtheid van CO₂ tot boven de tropopauze, resulteert een toename van dit gas niet tot fluxveranderingen in dit spectrale gebied. Vandaar de term verzadiging. De onverzadigde flanken van de 15 μm band zijn echter sterk genoeg voor een bijdrage van 90% in de totale stralingsforcering van CO₂.

- De verandering van stralingsfluxen door de toename van broeikasgassen kan als volgt worden geïnterpreteerd: de opwaartse straling aan de top van de atmosfeer wordt effectief van een grotere hoogte geëmitteerd. Gemiddeld is deze hoogte gesitueerd in de troposfeer, zodat een grotere hoogte correspondeert met een lagere temperatuur. Evenzo is de neerwaartse straling aan de grond effectief afkomstig van een lager niveau in de atmosfeer, dat gemiddeld op een paar honderd meter boven het aardoppervlak ligt. Hieruit blijkt dat de gemiddelde temperatuurafname met de hoogte cruciaal is voor het optreden van het versterkte broeikaseffect. Dit wordt bevestigd door onze analyse met het drie-parameter model van langgolvlige stralingstransport. De balans aan de top van de atmosfeer, die verstoord is door minder uitgaande langgolvlige straling in vergelijking met de netto binnenkomende zonnestraling, wordt uiteindelijk hersteld door een toename van de temperatuur van het aardoppervlak en de troposfeer, waardoor de opwaartse langgolvlige straling toeneemt. Dit staat bekend als het versterkte broeikaseffect.

In hoofdstuk 3 beschrijven we het breedbandige langgolvlige stralingsschema, dat voldoende efficiënt is om in een drie-dimensionaal klimaatmodel te worden gebruikt. Dit schema is gebaseerd op dat van *Morcrette* [1991] en is uitgebreid met de broeikasgassen CH₄, N₂O en 16 CFK's, HCFK's en HFK's, relevant voor klimaatstudies. Tevens hebben we de effecten van de 14 μm O₃ band [*Shine et al.*, 1995] en een nieuwe formulering van het waterdampcontinuum [*Giorgetta and Wild*, 1995] toegevoegd. In het kortgolvlige stralingsschema [*Fouquart and Bonnel*, 1980] zijn aanpassingen gemaakt voor de optische parameters van elf aërosol componenten,

gebaseerd op de Global Aerosol Data Set (GADS) [Koepke *et al.*, 1997]. Deze aangepaste lang- en kortgolvlige stralingsschema's zijn geselecteerd voor implementatie in het ECHAM4 klimaatmodel (MPI, Hamburg) [Roeckner *et al.*, 1996].

Het langgolvlige stralingsschema is geconstrueerd met behulp van fits van transmissiefuncties berekend met een smalbandig stralingsschema, waarin spectroscopische lijnparameters de basis vormen. Daarom vergelijken we tevens de stralingseffecten van drie verschillende spectroscopische databanken, namelijk HITRAN 1980, GEISA 1984, en HITRAN 1996.

Voorts evalueren we het langgolvlige schema met stralingsmetingen in Cabauw van de neerwaartse component nabij het aardoppervlak. Hiertoe worden profielen van temperatuur en vochtigheid, gemeten met de Cabauw mast (200 m), gecombineerd met radiosonde profielen in De Bilt. Hierbij worden ook de Brewer metingen van de totale hoeveelheid ozon gebruikt om een zo compleet mogelijk beeld te krijgen van de atmosferische condities, waaronder de stralingsmetingen zijn gedaan. Een selectie is gemaakt van 253 onbewolkte situaties, zodat alleen de geëmitteerde straling van broeikasgassen wordt vergeleken. Uit de evaluatie trekken wij de volgende conclusie:

- Gebruik makende van de meest recente spectroscopische parameters (HITRAN 1996) en de nieuwe waterdampcontinuum formulering, vinden we een goede overeenkomst tussen model en metingen met een correlatiecoëfficiënt van 0.99. Het gemiddelde verschil van -2 Wm^{-2} en de standaard afwijking van 4.2 Wm^{-2} liggen beide binnen de meetfout. Ook bij gebruik van de andere spectroscopische datasets liggen de verschillen tussen model en metingen binnen de meetfout. Verbetering van stralingsschema's kan worden bereikt door de spectrale resolutie te verhogen en door verbetering van de waterdampcontinuum formulering. De goede overeenkomst met de metingen geeft ons vertrouwen in de nauwkeurigheid van de stralingsforceringsberekeningen.

In hoofdstuk 4 berekenen we de stralingsforcering ten gevolge van veranderingen in troposferisch ozon en sulfaataërosolen, voor zowel de huidige situatie (1850-1990) als de toekomst (1990-2050). Aangezien de forcering van deze atmosferische bestanddelen met een relatief korte verblijftijd, en een daardoor inhomogene ruimtelijke verdeling, slecht bekend is, vormt de bepaling van hun stralingseffect een belangrijk thema in het huidige klimaatonderzoek. De concentratievelden van ozon en sulfaataërosolen alsmede van de gassen die leiden tot de vorming van deze bestanddelen, zijn bepaald met behulp van een drie-dimensionaal chemisch-transport model (MOGUNTIA) voor het preïndustriële tijdperk (1850), de huidige situatie (1990) en de toekomst (2050) op een $10^{\circ} \times 10^{\circ}$ rooster. Voorts hebben we een eerste schatting gemaakt van de stralingsforcering door nitraataërosolen. Tenslotte hebben we analytische fits voor de kortgolvlige forcering van troposferisch ozon en sulfaat afgeleid als functie van de oppervlakte-albedo en de zonnehoek. Deze analytische relaties kunnen gebruikt worden in drie-dimensionale modellen, waarvoor een geavanceerd stralingsschema te duur is. In hoofdlijnen kunnen de volgende

conclusies worden geformuleerd:

- De berekende mondiaal en jaarlijks gemiddelde stralingsforcering voor de industriële periode (1850-1990) is $+0.38 \text{ Wm}^{-2}$ en -0.36 Wm^{-2} voor de toename van respectievelijk troposferisch ozon en sulfaataërosol (direct effect). Deze waarden suggereren een balans. Echter, beide bestanddelen vertonen een eigen seizoenscyclus, terwijl ook hun forcering op een karakteristieke wijze afhankelijk is van allerlei stralingsparameters. Hierdoor ontstaan grote regionale en seizoensverschillen van de forceringspatronen van ozon en sulfaataërosol. Wanneer de stralingsforcering door de toename van homogeen gemengde broeikasgassen bij deze patronen opgeteld wordt, vertonen sommige industriële gebieden nog steeds een netto negatieve forcering. Dit wijst erop dat de effecten van sulfaataërosolen plaatselijk domineren. Op het noordelijk halfrond vinden we de sterkste gradiënten in de forceringspatronen in de zomer, vooral in de kuststreken. Dit zou consequenties kunnen hebben voor het regionale klimaat via dynamische terugkoppelingen.

- Op mondiale schaal is de forcering door nitraataërosolen een orde kleiner dan die door sulfaataërosolen. In sommige gebieden in Europa en de Verenigde Staten treden echter significant negatieve forceringen op. Voorts is een schatting gemaakt van de toekomstige forcering door troposferisch ozon en sulfaataërosol. De sterkste forceringen (positief voor ozon en negatief voor sulfaat) verschuiven naar gebieden met zich snel ontwikkelende economieën.

- Onze analytische fit voor sulfaataërosolen is een verbetering ten opzichte van de relatie van *Charlson et al.* [1991] waarin de oppervlakte-albedo de enige parameter is.

In hoofdstuk 5 analyseren we de relatieve bijdragen van diverse mechanismen, die mogelijk van invloed zijn geweest op de wereldgemiddelde temperatuur in de laatste 150 jaar. Hiertoe beschouwen we de antropogene component (broeikasgassen en sulfaataërosolen), de invloed van grote vulkaanuitbarstingen, en de mogelijke invloed van variaties in de zonneactiviteit. Om dit te bestuderen, gebruiken we het één-dimensionaal gekoppeld oceaan-atmosfeermodel. Zo'n klimaatmodel representeert de wereldgemiddelde eigenschappen van het klimaatstelsel, zoals de gemiddelde temperatuur- en vochtprofielen, bewolking, en energiebalans in de oceaan, aan het aardoppervlak, en in de atmosfeer. Voorts reageert het klimaatmodel op aangebrachte verstoringen in de stralingsbalans, bijvoorbeeld door een verandering van de samenstelling van de atmosfeer of door fluctuaties in de intensiteit van de binnenkomende zonnestraling. Dit soort verstoringen resulteren na enige tijd in temperatuurveranderingen. Deze vertraging wordt veroorzaakt door de grote warmteopslag (capaciteit) van de oceanen en is daarom sterk afhankelijk van de aard van de verstoring. Dit geldt eveneens voor de amplitude van de respons, de uiteindelijke temperatuurverandering nabij het aardoppervlak. Dit relatief simpele klimaatmodel is daarom zó afgeregeld dat de respons zowel qua amplitude als qua tijdsvertraging overeenkomt met de huidige generatie zeer complexe drie-dimensionale modellen, binnen

de bestaande onzekerheidsmarges. Vooral voor wat betreft de amplitude van de respons bestaat grote onzekerheid. Daarom gebruiken we ook een statistische techniek, analoog aan de kleinste-kwadraten methode, om de variaties van de onderzochte signalen zo goed mogelijk te laten samenvallen met de waargenomen temperatuurvariaties. Het voordeel van deze methode is dat we de amplitude van de diverse signalen kunnen afschatten zonder het fysisch mechanisme te kennen. De belangrijkste conclusies van hoofdstuk 5 zijn:

- Aan de hypothese van *Svensmark en Friis-Christensen* [1997] dat de elfjarige zonnevlekkencyclus via variaties in de kosmische straling de hoeveelheid bewolking moduleert, en daarmee een dominante invloed op het klimaat heeft, kleeft een aantoonbaar bezwaar: in de waargenomen temperatuurreeks zou in dat geval de zonnevlekkencyclus overheersend aanwezig moeten zijn. De waarnemingen spreken dit tegen: weliswaar komt een aantal van de elfjarige temperatuurfluctuaties overeen met de effecten van de zonnevlekkencyclus, maar vóór 1950 loopt het zonnevlekkensignaal uit fase t.o.v. het temperatuursignaal. Bovendien zijn de waargenomen lange-termijn temperatuurtrends aanzienlijk groter dan op grond van deze hypothese verwacht mag worden. Onze bevinding is dat de zwakke waargenomen elfjarige temperatuurschommelingen gedurende de laatste eeuw goed verklaard kunnen worden door de waargenomen variatie in de zonneconstante [*Lean*, 1991].

- De voorgestelde dominante invloed van lange-termijn variaties in zonne-activiteit [*Friis-Christensen and Lassen*, 1991], de zogeheten Gleissberg cyclus op een tijdschaal van circa 80 jaar, is ook onderzocht. We vinden dat dit signaal mogelijk verantwoordelijk is voor de waargenomen temperatuurstijging tussen 1910 en 1940 en gedeeltelijk voor de lichte afkoeling tussen 1940 en 1970. De temperatuurtoename sinds 1980 kan echter hoofdzakelijk worden toegeschreven aan de menselijke invloed op het klimaat. Al met al lijkt de bovengenoemde invloed van de zon op het klimaat, waarvoor in feite geen fysisch mechanisme bekend is, dus een goede verklaring voor de temperatuurfluctuaties eerder deze eeuw, tot dusver toegeschreven aan de interne variabiliteit. Ongeveer 88% van de waargenomen temperatuurvariaties sinds 1880 (waaruit de snelle jaar-tot-jaar fluctuaties weggefilterd zijn) kan verklaard worden door de menselijke invloed (40%), de elfjarige zonnevlekkencyclus (8%) en de Gleissbergcyclus (40%).

- Uit de berekende respons van antropogene en natuurlijke forceringsmechanismen vergeleken met de waargenomen wereld- en jaarlijks gemiddelde temperatuur sinds 1856, volgt dat de menselijke invloed op $+0.4 \pm 0.2$ K geschat kan worden.

- Simulaties met het één-dimensionale klimaatmodel laten een stratosferische afkoeling zien ten gevolge van de toegenomen emissie door broeikasgassen. Deze afkoeling treedt met name op in de $15\mu\text{m}$ band van CO_2 en is dus veroorzaakt door menselijke activiteiten. Bovendien reproduceert het model de buitensporige afkoeling in de lage stratosfeer sinds de zeventiger jaren, veroorzaakt door de trend in ozonafbraak [*Van Dorland and Fortuin*, 1994]. De berekende amplitude komt goed overeen met de waargenomen temperatuurafname van -0.4 ± 0.12 K per

decennium [Oort and Liu, 1993].

Toekomst

Het huidige klimaatonderzoek is uitgegroeid tot een multidisciplinair vakgebied. De voornaamste drijfveer van dit wereldomvattende onderzoek is de bezorgheid over het risico van snelle klimaatveranderingen in de komende eeuw, sneller dan de natuurlijke variaties sinds het eind van de laatste ijstijd, zo'n 12000 jaar geleden. De waargenomen temperatuurstijging van de laatste twee decennia past goed in dit beeld, maar onomstotelijk bewijs van de menselijke invloed kan nog niet gegeven worden. Daarom staan de relatieve bijdragen van antropogene en natuurlijke oorzaken aan de recente temperatuurstijging ter discussie. Soms leidt kritiek op het klimaatonderzoek zelfs tot volledige ontkenning van de menselijke invloed. In dit proefschrift komen twee controverses aan bod (zie hoofdstuk 2 en 5). Vaak leidt dit soort kritiek tot twijfel over het nut van het terugdringen van broeikasgasemissies.

Wij kunnen ons nu de fundamentele vraag stellen hoeveel bewijsmateriaal nodig is om de menselijke invloed op het klimaat aan te tonen. Tegen de tijd dat hierop antwoord mogelijk is, is het ongetwijfeld te laat voor maatregelen en wel om de volgende redenen: ten eerste betekent een sluitend bewijs van het versterkte broeikaseffect dat de mondiale verwarming een orde groter moet zijn dan de geschatte klimaatvariabiliteit uit waarnemingen en de bovengrens van mogelijke externe forceringsmechanismen. De klimaatvariabiliteit in de afgelopen eeuw is van de orde van 0.5 K. Ten tweede zal de ingezette verwarming op z'n minst een eeuw aanhouden door de atmosferische verblijftijden van de meeste broeikasgassen. Op dit moment moeten we bouwen op de huidige kennis van het klimaatsysteem, die nog verre van compleet is. De totale antropogene stralingsforcering wordt geschat op $+1.5 \pm 1.0 \text{ Wm}^{-2}$, waarbij de marge hoofdzakelijk veroorzaakt wordt door onzekerheid in de aërosolforcering.

Op grond van toekomstige emissie-scenario's mag verwacht worden dat in de volgende eeuw de effecten van broeikasgassen de koelende effecten van aërosolen ruimschoots zullen overtreffen. De totale stralingsforcering in 2100 wordt geschat op +4 tot +8 Wm^{-2} [IPCC, 1995]. We moeten hierbij aantekenen dat de huidige onzekerheid in de stralingsforcering niet in bovengenoemde marge verdisconteerd is. Doen we dit wel, dan komt de totale forcering in 2100 uit tussen de +1.5 en +13 Wm^{-2} . Wanneer we dit bereik vertalen naar temperatuurstijgingen nabij het aardoppervlak en ook de onzekerheid van een factor drie in de klimaatgevoeligheid verdisconteren, dan komen we uit op +0.5 K tot +14 K. De ondergrens is bij benadering gelijk aan de huidige geschatte klimaatvariabiliteit, terwijl de bovengrens een factor zeven groter is dan de temperatuurvariaties sinds het eind van de laatste ijstijd. Voorts weten we uit klimaatsimulaties met complexe drie-dimensionale modellen dat de temperatuurstijging ten gevolge van het versterkte broeikaseffect inhomogeen verdeeld is over de aardbol. Daarom lopen we een

groot risico met betrekking tot klimaatverandering door menselijke activiteiten, zelfs zonder de mogelijk onplezierige verrassingen door niet-lineaire klimaat-terugkoppelingen.

Maar hoe realistisch zijn bovengenoemde grenzen van de temperatuurstijging? Aangezien het produkt van stralingsforcering en klimaatgevoeligheid de mondiale temperatuurverandering bepaalt, moet het mogelijk zijn om uit temperatuurwaarnemingen in de komende decennia informatie te verkrijgen over de onder- en bovengrens van forcering en gevoeligheid. In feite hebben wij onze schatting van de huidige menselijke invloed, namelijk tussen de 0.2 K en 0.6 K, gebaseerd op de vergelijking met de waargenomen temperatuur. Voorts is het waarschijnlijk dat meer informatie over de menselijke invloed gehaald kan worden uit de combinatie van modeluitvoer en waarnemingen van de patronen van temperatuurverandering, de zogeheten vingerafdruk-methode [Santer *et al.*, 1996].

Vooralsnog moeten de onderzoeksinspanningen gericht zijn op het vernauwen van de onzekerheidsmarges van de directe en indirecte forcering van aërosolen. Verder is beter begrip van de veranderingen in de hydrologische cyclus, en in het bijzonder de rol van wolken hierin, noodzakelijk voor de bepaling van de klimaatgevoeligheid. Bovendien hangt het indirecte aërosoleffect samen met de microfysica van wolken. In dit opzicht kan vooruitgang geboekt worden door satelliet observaties en de ontwikkeling van retrieval-algorithmes voor ozon, aerosolen en wolken.

Hoewel geavanceerde drie-dimensionale gekoppelde oceaan-atmosfeermodellen nodig zijn voor een beter begrip van klimaatcycli en terugkoppelingsmechanismen, blijven stralingsschema's en simpele één-dimensionale klimaatmodellen nuttige hulpmiddelen bij het bepalen van de stralingsforcering en de daaruit voortvloeiende mondiaal gemiddelde temperatuurrepons van zowel antropogene als natuurlijke forceringsmechanismen.

Chapter 1

General Introduction

1.1 Motivation

By its various activities mankind is changing the composition of the earth's atmosphere. The steady increase of a number of greenhouse gases, such as carbon dioxide (CO₂), methane (CH₄), and nitrous oxide (N₂O), and of anthropogenic aerosols has become a major scientific and political issue during the past two decades. Unequivocal proof that climate change has already started as the result of increased greenhouse gas concentrations is not yet available. This is due to the presence of fluctuations of comparable magnitude in the past millenium, induced by interactions between the atmosphere, ocean, land, and cryosphere, and the impacts of volcanic eruptions and possibly solar activity. Although there exist large uncertainties in projections of global warming, we face a serious risk of widespread and longlasting effects. Especially, the rapidity of the expected climate change relative to natural climate variations since the last ice age, is reason for concern. This rapidity, in fact, determines the necessity for taking measures by governments, preferably world-wide, such as the reduction of greenhouse gas emissions and (further) development of alternative technologies to meet the energy needs of a growing world population. The multidisciplinary scientific community dealing with the investigation of climate change plays an important advisory role towards decision makers.

Since 1988 climate research efforts are collected within the framework of the Intergovernmental Panel on Climate Change [*IPCC*, 1990; 1992; 1994; 1995; 1997], aiming to publish comprehensive scientific reports including accessible summaries for policy makers, which are used in the worldwide negotiations to reduce the emission of greenhouse gases. At the present stage of climate research, using complex coupled ocean-atmosphere general circulation models and at the same time processing enormous amounts of data, measured by a number of monitoring satellites, ground-based instruments, radio sondes, airplanes etc., reflections are being made by the scientific community how to find evidence for the human influence on climate. Although our knowledge of the climate system is very incomplete, the complexity of the problem should not be used as an argument to have no concern about possible climate change due to human activities. Instead, efforts should be put in a further understanding of the climate system aiming to narrow the uncertainties.

Atmospheric radiative transfer is one of the most important processes in the climate system, because the only interaction of earth with outer space in terms of energy exchange takes place through radiation. In addition, all scenarios of climatic change are directly or indirectly

based on radiative feedback mechanisms. Radiative transfer is a process of transferring energy by electromagnetic waves. The sun is the primary source of energy for the earth's climate system. Globally and annually averaged, the climate system absorbs approximately 240 Wm^{-2} of shortwave (solar) radiation. Consequently, the climate system is heated and in turn produces longwave radiation. At least in the long term mean, the total radiative energy budget at top of the atmosphere, consisting of the net incoming solar radiation and the outgoing longwave radiation, has to be balanced.

This balance condition at the top allows the determination of the effective radiant temperature of our planet: equating the black body emission of the climate system to the net solar input, we obtain an effective temperature of about 255 K (-18°C). In an atmosphere only containing nitrogen and oxygen, while keeping the reflective properties of our planet unchanged, the mean surface temperature would be close to 255 K, i.e. the aforementioned effective radiant temperature. About 99% of the present atmosphere consists of nitrogen and oxygen. The remaining 1% of the atmosphere, which contains the so-called trace gases and water vapor, keep the planet at a habitable temperature of 288 K (15°C). The mechanism behind this warming is the so-called **natural greenhouse effect**.

On a global scale, perturbations of the radiation balance either in the longwave or in the shortwave part of the spectrum due to whatever cause, result in a climate change, since the energy balance at the top of the atmosphere is restored by changing the temperature of the earth's surface and the atmosphere. The best link between the radiative perturbations and subsequent surface temperature changes on a global scale, as can be derived from thermodynamic arguments, is given by the net flux change at the tropopause (on average at 13 km altitude). This net flux change is called the **radiative forcing**. Increases of greenhouse gases, which are mainly active in the longwave part of the spectrum, cause a positive radiative forcing and result in a warming of the climate system, known as the **enhanced greenhouse effect**. In contrast, increases of sulfate aerosols cause a cooling of the system due to their property of reflecting solar radiation, which is sometimes referred to as 'whitehouse effect'.

In this dissertation we focus on atmospheric radiative transfer and its change in the past one-and-a-half century. We are specifically interested in the determination of the radiative forcing, because on global scale this is an appropriate, but qualitative, indicator of the subsequent climate change. Therefore, we use a radiative transfer scheme, in which we incorporate all relevant constituents for climate studies. We evaluate this scheme with surface measurements of the downward longwave flux under clear sky conditions. In addition, we construct a 1D coupled ocean-atmosphere climate model, in which the radiative transfer scheme plays an essential role. We apply these models to calculate the radiative forcing and subsequent temperature responses due to a variety of anthropogenic and natural forcing mechanisms. In this thesis, we consider radiative forcing and climate change at the timescale of about a century for two reasons: in the first place, rapid changes in atmospheric composition due to human activities show up in the last century [IPCC, 1990; 1995]. Secondly, the time series of (global mean) temperature only

goes back until 1856 [Jones, 1994]. These temperature data are needed for a comparison with the computed temperature response on increasing levels of greenhouse gases and aerosols, using climate models, as well as for estimates of the natural variability of global temperature.

1.2 Outline of the Thesis

1.2.1 Radiation, Greenhouse Effect and Climate Change

Chapter 2 provides an introduction on radiation and climate. We give a brief overview on the historical perceptions of the greenhouse effect. In addition, the terminology and some basic notions on interactions between matter and radiation applied to atmospheric radiative transfer are described. We explain the link between radiative forcing and subsequent surface temperature changes, based on thermodynamic arguments in relation to the typical temperature structure of the global mean atmosphere. This temperature structure is tightly connected with the presence and vertical distribution of radiatively active constituents in the atmosphere. Therefore, we also discuss the globally and annually averaged energy balance of the climate system. Furthermore, we simplify the radiative transfer equation in order to reveal the most important parameters responsible for the mechanism of enhanced greenhouse effect. The solutions of the analytical model are verified and compared with the general characteristics of the upward and downward radiative fluxes as calculated with the broad band radiative transfer scheme, described in Chapter 3. Since the transparency of the background atmosphere has a dominant impact on the typical profiles of longwave radiative transfer, we separate the radiative fluxes into the transparent window region and the rather opaque remainder of the spectrum. Here, we also consider the radiative effects in the saturated center of the $15\ \mu\text{m}$ band of CO_2 . It will be shown further that the decrease of temperature with height is of utmost importance for the occurrence of the enhanced greenhouse effect. Conclusions based on this simple analytical model are used to explain high spectral resolution radiative transfer computations. Furthermore, we pay attention to the consequence of perturbations in the radiation balance, which is climate change. We discuss the central questions in climate research, the possible causes of climate change, the models used in this field of research and the present uncertainties associated with the changing composition of the atmosphere due to human activities.

1.2.2 Radiative Transfer Scheme

In Chapter 3 we describe the longwave radiative transfer scheme for climate modelling purposes, which is sufficiently computationally efficient to be incorporated in a General Circulation Model (GCM). The scheme is based on the *Morcrette* [1991] scheme and extended with the greenhouse gases CH_4 , N_2O and 16 CFCs, HCFCs and HFCs, which are relevant for climate studies. Also, we incorporate the $14\ \mu\text{m}$ band of ozone, since this absorption band contributes significantly to radiative transfer, especially in the stratosphere [Shine *et al.*, 1995]. Furthermore, we include

a new formulation of the water vapor continuum [Giorgetta and Wild, 1995]. In the shortwave scheme [Fouquart and Bonnel, 1980] adaptations are made for the optical parameters of eleven aerosol components based on the Global Aerosol Data Set (GADS) [Koepke et al., 1997]. The longwave and shortwave radiative transfer schemes have been selected to be part of the ECHAM4 climate model (MPI, Hamburg) [Roeckner et al., 1996].

We show how to construct the longwave wide band scheme from fits of the transmission functions as calculated with a high spectral resolution scheme. Spectroscopic line information of the individual greenhouse gases present in the atmosphere is processed into absorption parameters for the narrow band scheme, based on [Morcrette and Fouquart, 1985], using statistical band models. We make a comparison of the impact on radiative transfer using three compilations of spectroscopic line parameters, namely HITRAN 1980 [Rothman, 1981], GEISA 1984 [Husson et al., 1986] and the most recent one, HITRAN 1996 [Rothman et al., 1998].

In addition, we evaluate the wide band scheme with longwave surface radiation measurements at Cabauw in the Netherlands. As input for the scheme we combine the atmospheric profiles of temperature and humidity from the Cabauw tower (200m) with rawind sonde measurements at De Bilt (up to about 30 km). We also include total column ozone information, measured with the Brewer spectrophotometer in De Bilt. Excellent agreement is found between measurements and the radiative transfer calculations within the range of measurement errors. Therefore, we have confidence in the performance of our constructed scheme for climate modelling purposes [Van Dorland, R., P. Stammes, A.A.M. Holtslag, and W. Kohsiek, *A longwave radiative transfer scheme for climate modelling and its evaluation with surface observations at Cabauw*; submitted to *Quart. J. Roy. Met. Soc.*, 1999].

1.2.3 Climate Studies

In Chapter 4 we discuss the radiative forcing due to changes in tropospheric ozone and sulfate aerosols at present (1850-1990) as well as for the future (1990-2050). Since the radiative forcing due to these relatively short-lived and therefore inhomogeneously distributed constituents exhibits a large degree of uncertainty, the determination of their effects is one of the highlights in present climate research. The concentration fields of ozone and sulfate aerosols and their precursors on a $10^{\circ} \times 10^{\circ}$ grid are computed with a three-dimensional transport/chemistry model (MOGUNTIA [Zimmermann, 1987]) for the pre-industrial (1850) case, the contemporary atmosphere (1990) and for the future (2050). For sulfate aerosols we determine the impact of relative humidity on the radiative forcing. Relative humidity determines largely the size distribution of these particles, which has implications for the optical parameters and thus for the reflected solar radiation. Also, we present analytical fits for the shortwave component of the radiative forcing of ozone and sulfate aerosols so as to show the dependencies on the solar zenith angle and surface albedo [Van Dorland, R, F.J. Dentener, and J. Lelieveld, *Radiative forcing due to tropospheric ozone and sulfate aerosols*, *J. Geophys. Res.*, 102, 28,079-28,100, 1997].

In Chapter 5, we make an assessment of the possible forcing mechanisms in the last century. Therefore, we develop a 1D coupled ocean-atmosphere Radiative-Convective Model which includes the aforementioned radiative transfer scheme, aiming to perform transient global mean climate simulations with respect to the temperature response. With the help of a statistical method, we make an attempt to attribute these causes of climate change by comparing model results with the observed global mean temperature, which goes back until 1856 [Jones, 1994]. As input for the model we adopt the increases of greenhouse gas concentrations as a function of time since 1850. Also, we incorporate the evolution of the estimated direct as well as indirect effect of sulfate aerosols. Apart from this anthropogenic signal, we vary the stratospheric sulfate content due to large volcanic eruptions in the last one-and-a-half century, using the volcanic dataset of Sato *et al.* [1993]. Furthermore, we test recent hypotheses concerning the climate perturbations of the 11-year sunspot cycle as well as variations of the length of this cycle on a timescale of about 80 years, the so-called Gleissberg cycle [Van Dorland, R., and A.P. van Ulden, *Natural and anthropogenic variations in the radiation balance, proceedings Sun and Climate: the influence of variations in solar activity on the earth's climate*, 1998].

In Chapter 6, we summarize the subjects and main conclusions of the successive chapters of this dissertation. Also, we present our outlook on climate research, with respect to the present status and possibilities for directions of future research, aiming at the detection and attribution of the human influence on climate in the next century. Based on our atmospheric radiative transfer and greenhouse effect studies, we express our concern of the serious risk of global warming by which we put a burden upon the next generation with a possibly huge problem.

Chapter 2

Atmospheric Radiative Transfer, Greenhouse Effect and Climate Change

2.1 Introduction

As an introduction to the subject of this thesis, some basic elements in the understanding of atmospheric radiative processes, the mechanism of the greenhouse effect, and climate change are presented. Besides the selected items, which can be found in textbooks on either radiation or climate change, we aim to present our view on the global mean energy balance, using a combination of observations and computations with the radiative transfer scheme, used in this dissertation (for documentation see Chapter 3). In addition, we offer our approach towards the analysis of the (enhanced) greenhouse effect in relation to the (increase of) longwave radiatively active gases, while accounting for the location of their most important absorption bands in the spectrum. Since radiative transfer plays an essential role in the energy balance of the climate system as well as in the determination of climate change, it appears appropriate to seek answers on the following five questions, giving also structure to the successive sections in this chapter.

1. How did the knowledge of the greenhouse effect evolve? Knowledge about the historical concepts in this field of research is useful to recognize present ideas and criticism. Moreover, previous attempts to verify or falsify physical concepts through either experimental data or theoretical considerations often clarify much more than reading publications on the present status of research in which underlying principles are taken for granted. The historical line is one of growing recognition of the importance of radiation processes in the climate system.

2. What do we know about atmospheric radiation? Climate models make use of radiative transfer schemes which are heavily parameterized in order to be computationally efficient [Ellingson *et al.*, 1991; IPCC, 1995]. These schemes are based on theoretical concepts describing the interactions between matter and radiation, applied to the earth's atmosphere [Goody and Yung, 1989]. In addition, ground based and satellite measurements are available to validate outputs of climate models and radiation schemes [Ramanathan, 1987; Rossow and Zhang, 1995; Garratt and Prata, 1996; Wild *et al.*, 1997; Chapter 3].

3. What do we know about the global energy balance? Although the only interaction between the climate system and outer space takes place through radiation, non-radiative energy

flows such as latent and sensible heat, have a large impact on the surface as well as on the tropospheric energy balance. With respect to the global and annual mean balance, tendency terms related to horizontal advection of heat by dynamical processes cancel out, simplifying greatly our picture of the average world. This can be made very useful in defining and describing the general features of climate change, using simple 1D climate models (Chapter 5), which represent only the most critical processes as identified by complex models [IPCC, 1997].

4. What determines the mechanism of the enhanced greenhouse effect? For the understanding of this mechanism, it is useful to determine a minimum set of parameters, which can describe the characteristics of atmospheric radiative transfer as well as the changes therein due to increases of greenhouse gases. Since these gases are essentially active in the infrared part of the spectrum, it appears to be sufficient to limit ourselves to the longwave radiative transfer equation. Much of the criticism on current research of climate change due to human activities can be traced back to a misinterpretation of the mechanism of the enhanced greenhouse effect, putting emphasis on the changes in the surface energy balance [Idso, 1980; Emsley, 1994; Barrett, 1995; ESEF, 1996] instead of making an assessment of the changes at levels which are more relevant in a thermodynamical sense [Mitchell, 1989; Ramaswamy, 1991; Van Dorland, 1995; Van Dorland, 1997].

5. How do we study climate change? The central question in climate research is how much of the warming trend in the observed temperature of the last one-and-a-half century can be attributed to the human influence. At present, complex coupled ocean-atmosphere general circulation models are used to study the climate system. The merits of these models lie in resolving regional climate changes, although there is a considerable degree of disagreement between these complex models on the regional scale. However, in this chapter we point out that simpler models are useful tools to determine at least qualitatively global mean temperature changes due to imposed forcing mechanisms.

In section 2.2, we give a brief overview on the historical perceptions of the greenhouse effect, starting in the early nineteenth century. This section is followed by a description of the interaction between matter and radiation, in which the basic terminology, black body radiation and the general structure of the radiative transfer equation are explained (section 2.3). For further details and references, the reader is referred to textbooks, e.g. *Goody and Yung* [1989], *Paltridge and Platt* [1976], *Liou* [1980], *Lenoble* [1993]. In section 2.4 the global energy balance is discussed. The general temperature structure of the global mean atmosphere is tightly connected with the presence and vertical distribution of radiatively active constituents as well as with latent and sensible heat flows in the troposphere. This temperature structure appears to be crucial for the mechanism of the enhanced greenhouse effect. Also, the concept of radiative forcing and its connection with surface temperature change are described from a thermodynamic point of view. By removing atmospheric constituents successively in a simple 1D climate model, we

estimate their relative importance in the global energy balance. In section 2.5, an analytical (three-parameter) model for longwave radiative transfer characteristics in the troposphere is presented. The results are compared qualitatively with the radiative fluxes calculated by the sophisticated broad band radiative transfer scheme, described in Chapter 3. Using this analytical model, the general characteristics of the enhanced greenhouse effect can be derived. In section 2.6 we pay attention to the central questions in climate research, the possible causes of climate change, the models used in climate research, and the present uncertainties associated with the changing composition of the atmosphere due to human activities. In section 2.7, we summarize the most relevant conclusions of this chapter.

2.2 Historical Perceptions of the Greenhouse Effect

2.2.1 Concepts in the Nineteenth Century

In the early nineteenth century, Jean Baptiste Joseph Fourier, most famous for his Fourier series, may be considered as the scientist who brought up the subject of the now well-known greenhouse effect for the first time [Fleming, 1998]. Fourier's paper *Mémoire sur les températures du globe terrestre et des espaces planétaires* [1827] is basically a discourse on the temperature regimes of the atmosphere, the surface and the interior of the earth. His motivation was to seek an explanation for the habitable surface temperatures. In the concept of Fourier, the atmosphere behaves like a transparent glass cover of a box, exposed to the sun, by allowing the shortwave radiation to penetrate to the earth's surface. The 'obscure' radiation, which is another term for the longwave radiation as it is invisible to the human eye, originates from the earth's surface as a conversion of the solar beam and is retained partially in the atmosphere, which is warmed subsequently.

In 1861 John Tyndall performed laboratory measurements of the absorption properties of water vapor and atmospheric gases, such as carbon dioxide. In his work *On the absorption and radiation of heat by gases and vapours* [1861], he credited Fourier with the notion that the interception of terrestrial rays has an important influence on climate. Tyndall suggested further that changes in the amount of radiatively active gases in the atmosphere could have produced 'all the mutations of climate which the researches of geologists reveal'. In fact, he was the first who demonstrated that some of the trace gases in the atmosphere were active absorbers and emitters of heat radiation, at least in the infrared. This may be considered as an essential adjustment of Fourier's theory, who did not discriminate between the constituents of the atmosphere with respect to their longwave radiative properties.

Quantitative statements on the greenhouse effect were made by Svante Arrhenius in 1896 in his publication *On the influence of carbonic acid in the air upon the temperature of the ground*. Calculations were performed for estimating the temperature change due to changes of the CO₂ concentration and were aimed to show possible climate changes during the ice-ages due to carbon dioxide fluctuations [Rodhe and Charlson, 1998]. For a doubling of the CO₂ concentration

Arrhenius computed a surface temperature change of about 4-6 K, which is an overestimate, but of the same order as computed with the comprehensive 3D climate models used by the scientists nowadays. In addition, Arrhenius' calculations reveal the logarithmic relationship between fluctuations of the CO₂ concentration and the subsequent temperature changes. Arrhenius had become aware of the rapid increase in anthropogenic carbon emissions. However, he thought that burning fossil fuels could help to prevent a rapid return to the conditions of an ice age, as well as to be beneficial for mankind due to the stimulation of plant growth and hence providing more food for a larger population. Therefore, his point of view differs from the present one, which is dominated by the concern about harmful effects of increasing CO₂.

2.2.2 Developments in the Twentieth Century

Up to 1950, most scientists were not concerned about a possible global warming due to increasing CO₂ concentrations. It was widely believed, on the basis of false criticism of Arrhenius' view, that at the then present atmospheric concentrations of water vapor and carbon dioxide all longwave radiation was already absorbed, known as saturation. Hence, any further increase of CO₂ would not affect the global energy balance significantly, but stimulate plant growth instead, a view which has some support up to now [ESEF, 1996]. This belief in CO₂ saturation was based on laboratory experiments performed by K. Ångström at the beginning of the century, in which he measured the absorption of longwave radiation in tubes filled with air samples. Hence, Arrhenius' ideas on climate change were overruled by the misinterpretation of radiation measurements by Ångström.

As global temperatures had increased between 1910 and 1940, Callendar [1938] focussed on the possible link between anthropogenic CO₂ emissions and climate warming. However, wider attention in the scientific community came more than ten years later in the 1950s. Concerns about global warming and its consequences, such as sea level rise, loss of habitat and possible shifts of agricultural zones, were expressed in both the scientific [Revelle and Suess, 1957] and popular press. This resulted after the International Geophysical Year (1957) in routine measurements of the CO₂ concentration at Mauna Loa, Hawaii.

The technical progress, especially the introduction of the computer, allowed Plass [1956] to apply the fundamentals of atmospheric radiative transfer in numerical models. Also, databases were constructed of the spectroscopic line parameters of greenhouse gases in the earth's atmosphere and used in radiative transfer models [Yamamoto, 1952; Howard *et al.*, 1955]. In the 1960s, S. Manabe, R.T. Wetherald and R.F. Strickler can be considered as pioneers of the modern research on climate change. In fact, the first climate models were 1D radiative-convective models in which the vertical structure of the atmosphere was resolved in order to compute atmospheric radiative transfer together with the fast convective redistribution of energy in the surface-troposphere system [Manabe and Strickler, 1964]. These models were used to show the equilibrium response due to instantaneous increases of CO₂ with and without some climate

feedbacks. Later on, extensions were made to 2D climate models, in which the equator to poles heat transports were parameterized [Manabe and Wetherald, 1967].

In the 1970s, computers were powerful enough to develop 3D general circulation models for climate research, although with very coarse resolution [Manabe and Wetherald, 1975]. Simultaneously, satellites were equipped with instruments, which could monitor the outgoing longwave and the reflected shortwave radiation from the earth-atmosphere system. After about ten years of 3D modelling by several research institutes, the Intergovernmental Panel on Climate Change (IPCC) was founded (1988) in order to assess the scientific achievements with respect to climate change. In the first report [IPCC, 1990] emphasis was put on equilibrium climate response due to increases of greenhouse gases mainly. In the last decade, the 3D climate models have been coupled to sophisticated ocean models and equipped with modules in which atmospheric chemical processes are computed, aiming at the calculation of transient responses, climate variability as well as the incorporation of radiatively active short-lived constituents, such as ozone and aerosols [IPCC, 1995]. Also, a start has been made to incorporate biospheric modules in climate models. Therefore, the science of climate change has grown into a multidisciplinary field of research.

2.3 Interaction between Matter and Radiation

2.3.1 Terminology

Radiation is a process of emitting, transferring or receiving electromagnetic energy. From a quantumphysical point of view these electromagnetic waves can be interpreted as the probability field related to light quanta or photons. The frequency ν of an electromagnetic wave is a measure of the energy $E = h\nu$ of the photon and vice versa. The conversion factor is Planck's constant h . Similarly, particles are associated with probability fields as well. Most conveniently, interactions between matter and radiation are described in terms of energy exchange between photons and molecules, rather than in terms of the interference of their associated probability fields.

The most basic measure of the quantity of radiation flowing in a given direction is **specific intensity** or **radiance**, $L(P, \mathbf{s})$ expressed in $\text{Wm}^{-2}\text{sr}^{-1}$, and is defined as the total radiant energy, E (in J), at point P in a given direction \mathbf{s} , per unit time t , per unit solid angle ω , and per unit area A (surrounding point P) perpendicular to the given direction: $E = L(P, \mathbf{s})dAd\omega dt$.

The **radiant energy density** of the photon field, $u(P)$, is calculated by integrating the radiance over all directions, i.e. a solid angle of 4π , divided by the velocity of light c , and is expressed in Jm^{-3} . The concepts of **radiant emittance** and of **irradiance** are complementary in that they are both measures of the areal density of the radiant flux referred to source and receiving surface, respectively. The term **flux density**, F , (or shortly **flux** in this thesis) is used in reference to either one and is expressed in Wm^{-2} [Paltridge and Platt, 1976]. Flux densities are obtained from radiances by integrating them over half-spheres, commonly for surfaces in a horizontal plane. Radiative transfer calculations within atmospheric circulation models for weather

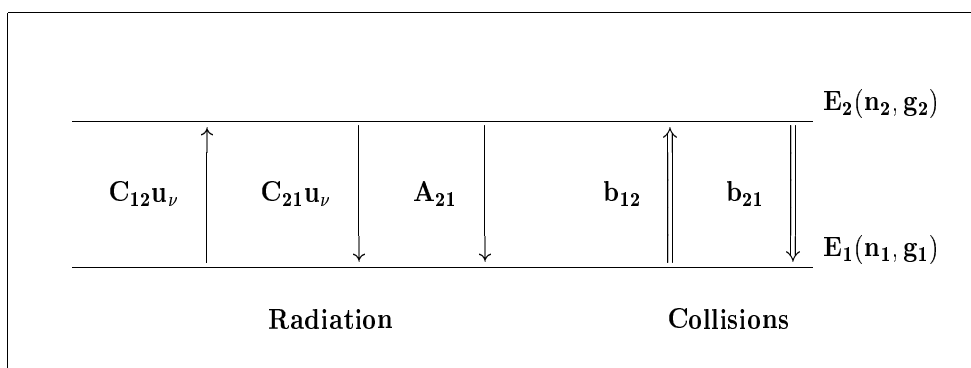


Figure 2.1: Transitions involving two energy levels, $E_2(n_2, g_2)$ and $E_1(n_1, g_1)$, where n_i and g_i ($i = 1, 2$) are the state populations and the statistical weights, respectively. A_{21} , C_{12} and C_{21} are the Einstein coefficients for radiative transitions. A_{21} is the probability per unit time of spontaneous emission, $C_{12}u_\nu$ and $C_{21}u_\nu$ the probabilities per unit time of absorption and induced emission, respectively. b_{12} and b_{21} are the collisional transition coefficients.

and climate aim to compute the **radiative tendency**, i.e. the rate of temperature change due to the vertical divergence of the net flux.

All these quantities have their counterpart when referred to monochromatic radiation, i.e. radiation confined to a specific and infinitesimal interval of frequency (or wavelength), being spectral quantities denoted by the subscript ν , e.g. spectral energy E_ν , spectral radiance L_ν and spectral flux F_ν . The radiation field, if polarization is not considered, is fully characterized if at any point $P(\mathbf{x})$ for any direction \mathbf{s} at any time t we know the radiance $L_\nu(\mathbf{x}, \mathbf{s}, t)$ for each frequency ν . Special cases of the radiation field are isotropic radiance (no dependence on the direction \mathbf{s}), homogeneous radiance (no dependence on point $P(\mathbf{x})$) and stationary radiance (constant in time). For a horizontally homogeneous radiation field, the radiance is only dependent on height or any other suitable vertical coordinate.

All matter which will be considered here, i.e. which is essential for atmospheric radiative transfer, has electronic, vibrational and rotational energy and in case of gases (and fluids) also translational internal energy. Interaction between radiation and matter takes place when the energy of a photon is either transferred to or released by a molecule or an atom. Extinction takes place when a photon's energy is transferred to matter, lifting the atom or molecule to a higher energy state (coefficient $C_{12}u_\nu$ in Figure 2.1), hence proportional to the incident radiant energy density. This received energy can be returned to the field of radiation in several ways: in case of spontaneous release (coefficient A_{21}), usually taking place within 1 ns, matter returns to its original state either directly or via a cascade of intermediate energy levels. If the photon changes its direction, the intensity of the photon field in the original direction is reduced, but the field in the direction of the outgoing photon benefits. This process is called **scattering**

and is conservative for the radiation field as a whole. If during the excited state of a molecule a collision with other molecules takes place, causing a return to its original state (coefficient b_{21}), the energy is transferred to other forms of internal energy. In case of complete thermodynamic equilibrium this energy is shared among all the accessible degrees of freedom (so-called equipartition). Where energy is transferred to the kinetic energy (translational energy) of the colliding molecules, resulting in an increase of the temperature of the volume containing these molecules, the process is called **absorption** and reduces the total radiative energy since the photon is actually lost. Collisions can also raise the energy level of a molecule (coefficient b_{12}), and trigger the release of photons. If applied to a large number of colliding molecules, this process is called **thermal emission**, as kinetic energy is converted into radiative energy. The third form of radiative transitions is **induced emission**, which is influenced by the incident radiation field and hence proportional to the radiant energy density (coefficient C_{21u_ν}). The release of photons due to induced emission takes place in the direction of incidence, whereas spontaneous emission is isotropic by virtue of the random process.

2.3.2 Black Body Radiation

Black body radiation is the radiation occurring inside a constant-temperature enclosure or cavity, if matter (i.e. the walls of the cavity) and radiation are in a state of complete thermodynamic equilibrium. Most solids and liquids are able to absorb all longwave radiation fairly uniformly with respect to frequency, a consequence of the dense packing of molecules and atoms. As a first order approximation they may be considered as black bodies with respect to longwave radiation, e.g. which holds for the earth's surface. The spectral distribution of black body radiation was first derived by Planck in 1900. As a consequence of the thermodynamic equilibrium it is a function of temperature T only. The spectral radiance of a black body is given by:

$$L_\nu^B(T) = \frac{2h\nu^3}{c^2[\exp(h\nu/kT) - 1]}, \quad (2.1)$$

where $h=6.62559 \times 10^{-34}$ Js is the Planck constant, $k=1.38020 \times 10^{-23}$ JK⁻¹ is the Boltzmann constant, and $c=2.99793 \times 10^8$ ms⁻¹ is the velocity of light in vacuum. In fact, Planck's ad hoc concept of discrete energy states in order to derive the spectral radiance emitted by a black body resulted in the origin of quantumphysics.

The Planck function (Eq.2.1) implies that black body radiation increases with temperature for each wavelength or frequency. Moreover, it has a single maximum, which is dependent on temperature (Figure 2.2). The wavelength where the maximum of the spectral black body radiation occurs is given by Wien's displacement law:

$$\lambda_{max}T = 2.8978 \times 10^{-3}mK \quad (2.2)$$

This implies that the Sun, with its radiant temperature of 6000 K, as an approximate black body, has its maximum for a wavelength of 0.5 μ m, while only 0.4% of its energy has wavelengths

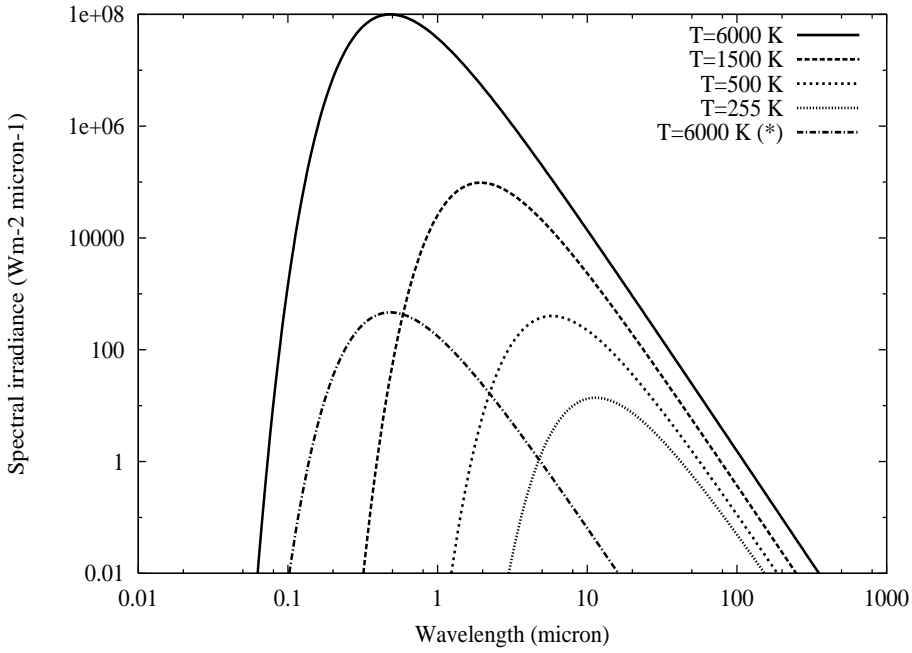


Figure 2.2: Planck curves of black body radiation in terms of irradiance for four temperatures, 6000 K (sun), 1500 K, 500 K, and 255 K (effective temperature of the earth-atmosphere system). For comparison also the curve is shown for the average solar irradiance at the top of atmosphere (which is a quarter of the solar constant if spectrally integrated), denoted by $T=6000\text{ K} (*)$.

longer than $5\ \mu\text{m}$. For typical atmospheric and surface temperatures around 250 K, the maximum occurs for $10\ \mu\text{m}$, while only 0.4% of its energy is emitted for wavelengths shorter than $5\ \mu\text{m}$ [Goody and Yung, 1989]. At the sun-earth distance, the cross over point of incoming solar radiation and outgoing longwave radiation occurs for a wavelength of about $5\ \mu\text{m}$ (Figure 2.2). This facilitates the separate treatment of solar and terrestrial radiation in radiation models.

By integrating the spectral radiance of a black body over the entire spectrum, we get the Stefan-Boltzmann radiation law:

$$L^B(T) \equiv \int_0^\infty L_\nu^B d\nu = \frac{2\pi^4 k^4}{15c^2 h^3} T^4 \equiv \frac{\sigma}{\pi} T^4, \quad (2.3)$$

where $\sigma = 5.6697 \times 10^{-8}\ \text{Wm}^{-2}\text{K}^{-4}$ is the Stefan-Boltzmann constant, which can be expressed in basic physical constants. Since black body radiation is isotropic by definition, angular integration over a half-sphere results in a total emitted flux of $F \equiv B = \sigma T^4$, expressed in Wm^{-2} .

In contrast to most solids and liquids, the absorption and emission by atmospheric gases is highly selective with regard to frequency. In the far infrared ($>20\ \mu\text{m}$) absorption lines are well separated and are related to the transition between two discrete rotational states. For shorter

wavelengths (between 1 μm and 20 μm) the coexistence of rotational and vibrational transitions leads to a very complex structure of absorption lines, which partially overlap each other. In the visible spectrum and at higher frequencies transitions between electronic states occur on top of the other energy transitions. Basically, these spectral properties of gases imply that the atmosphere may not be considered as a black body emitter and so its ‘blackness’ is strongly dependent on the spectral region considered and on the density of the radiatively active molecules in the atmosphere.

Generally, matter absorbs a fraction α_ν of the incident spectral radiance at frequency ν . If $\alpha_\nu = 1$, the material is black in the usual sense, at least for frequency ν , and it emits black body radiation. In thermodynamic equilibrium, the ratio of the emitted radiance to the black body radiance at the same temperature is defined as the **emissivity** ϵ_ν , which is equal to the **absorptivity** α_ν . This fundamental principle is known as Kirchhoff’s law.

2.3.3 Radiative Transfer Equation

The interactions between matter and radiation can be classified as either **extinction** or **emission**. The two processes are distinguished by the sign of the radiance change. For a decrease in radiance we have extinction, whereas for an increase we use the term emission. Extinction can be considered as the sum of absorption and scattering. If we consider the change of spectral radiance along path ds , any change in the intensity at point $P(\mathbf{x})$ in the direction \mathbf{s} resulting from the interaction between matter and radiation can be written as the sum of the change by extinction and emission, which is known as the radiative transfer equation (RTE) [Goody and Yung, 1989]:

$$\mathbf{s} \cdot \nabla L_\nu(P(\mathbf{x}), \mathbf{s}) = -e_{\nu, \nu} [L_\nu(P(\mathbf{x}), \mathbf{s}) - J_\nu(P(\mathbf{x}), \mathbf{s})] \quad (2.4)$$

where L_ν is the spectral radiance, $e_{\nu, \nu}$ is the volume extinction coefficient and J_ν is defined as the spectral **source function**. The ∇ operator operates on the position vector \mathbf{x} of P .

Extinction, appearing as the first term at the right-hand-side of the RTE, is described by the Lambert-Beer law. To satisfy this law, the coefficient $e_{\nu, \nu}$ must be proportional to the local density of absorbing matter. Possible nonlinear effects, e.g. for very high photon densities, are not considered here, because they are unimportant for atmospheric radiative transfer. The argument that the extinction process is linear in the amount of matter applies with equal force to the emission process (second term at the right hand side of the RTE). Furthermore, emission is proportional to the source function J_ν . The physics of radiative transfer is mainly contained in the determination of the extinction coefficient and the source function.

Atmospheric conditions greatly simplify the RTE for two reasons. Firstly, the solar spectrum is well separated from the infrared spectrum as discussed in section 2.3.2. In the solar part we may neglect thermal emission. Therefore, the source function for solar radiation is completely determined by scattering processes by molecules (Rayleigh scattering) and cloud droplets as well as aerosols (Mie scattering). In the infrared spectral region we may neglect

scattering. Rayleigh scattering is inversely proportional to the fourth power of the wavelength and can therefore be neglected completely in this part of the spectrum. Whereas the neglect of droplet scattering can be justified by the fact that within clouds there is an abundance of water vapor, which rapidly absorbs photons penetrating the cloud. This is reinforced by the fact that photons are preferentially scattered in forward direction for the Mie scattering process [Ritter, 1986]. Therefore, in the infrared spectrum the extinction coefficient reduces approximately to an absorption coefficient.

Secondly, the air is sufficiently dense up to an altitude of about 50 km to be in a state of **local thermodynamic equilibrium**. Under such conditions the collisional rates are much higher than the rates of spontaneous emission, which are the inverse of the natural lifetimes of the excited states with respect to radiative transitions [Goody and Yung, 1989; Lenoble, 1993]. Einstein demonstrated that in this case, for which the most relevant energy levels of the molecules still obey Boltzmann's law at local temperatures, the source function is given by Planck's law (Eq.2.1). Therefore, in the infrared spectral region the product of the absorption coefficient and the Planck function or black body radiation determines the thermal emission. Of utmost importance is the fact that both absorption and emission are proportional to the absorption coefficient, which is highly selective with regard to frequency.

The absorption coefficient itself is dependent on temperature and pressure, both through the line strength and width. Especially weak lines show strong increases of their strength with temperature as will be explained in Chapter 3 (Appendix). In the lower atmosphere, up to about 40 km, absorption lines are broadened by the many collisions, resulting in a Lorentzian line shape. Higher up in the atmosphere, Doppler effects resulting from the thermal velocity of atoms and molecules are responsible for the broadening of the absorption lines. These broadening effects in the atmosphere thus result in a non-monochromatic character of gaseous absorption lines. The width of the absorption lines having a Lorentzian shape is proportional to the collision frequency. Using some simplifying assumptions about the shape and size distribution of the molecules, it can be shown that the Lorentz widths of the lines are proportional to the pressure and inversely proportional to the square root of the temperature [Ritter, 1986]. This implies that on average, the effectiveness of absorption and emission as compared to black bodies decreases with altitude due to the aforementioned temperature and pressure dependencies.

2.4 Global Energy Balance and Radiative Forcing

2.4.1 Global Energy Balance

Atmospheric radiative transfer is one of the most important features in the climate system, because the only interaction with outer space in terms of energy exchange takes place via radiation. The sun is the primary source of energy for the earth's climate system. According to the latest measurements, the solar flux at the mean sun-earth distance has a value of 1370 Wm^{-2} , known as the solar constant. The global energy balance is shown in Figure 2.3. The figure is based

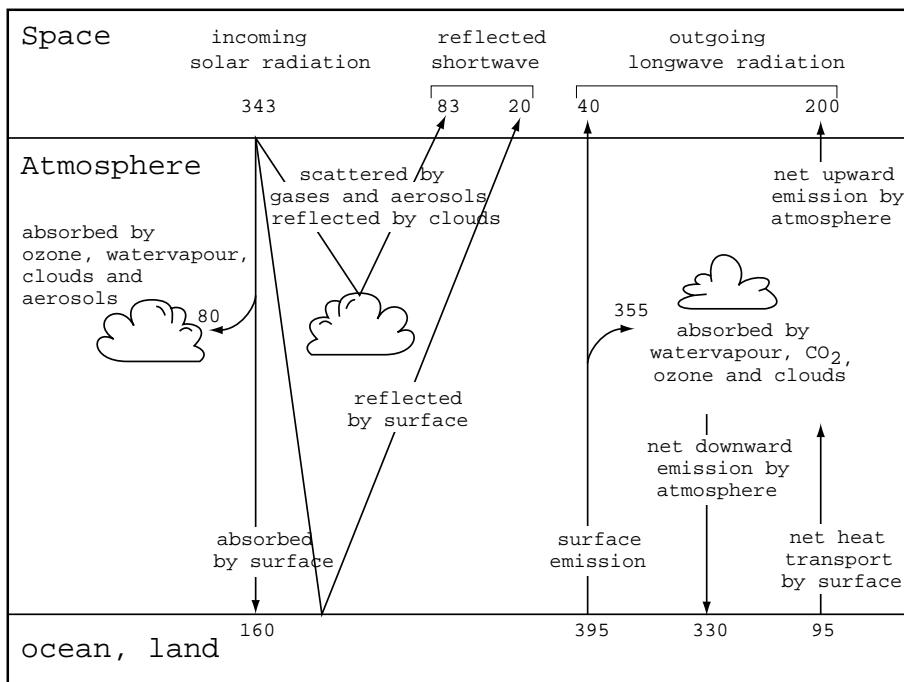


Figure 2.3: Global and annual mean energy balance of the climate system (Unit= Wm^{-2}).

on measurements and computations by the Radiative-Convective Model described in Chapter 5. On average, the globe is illuminated effectively by the solar constant times $\frac{1}{4}$, being the ratio between the cross section of the earth, perpendicular to the solar insolation, and the earth's total surface. The shortwave radiation, originating from the sun is either absorbed, scattered or reflected in the atmosphere or at the surface of the earth. The ratio between reflected and incident irradiance at the top of the atmosphere, the so-called planetary albedo, has been measured by satellites to be around 0.3. Therefore, the true global and annual mean solar input to the earth-atmosphere system is approximately $240 \pm 5 \text{ Wm}^{-2}$. Most of the shortwave radiation, $160 \pm 10 \text{ Wm}^{-2}$, reaches the earth's surface and is absorbed by the oceans and land-masses; observations show that about $80 \pm 10 \text{ Wm}^{-2}$ is absorbed in the atmosphere by ozone, water vapor, clouds and aerosols [Ellingson and Fouquart, 1990; Cess et al., 1995; Pilewskie and Valero, 1995]. There is still some debate on the amount of absorbed shortwave radiation by clouds. This explains largely the uncertainty in this value [Zhang et al., 1997].

The present global and annual mean temperature of the earth's surface is approximately 289 K. Due to the fact that the atmospheric temperature decreases with height, the thermal emission towards the surface, $330 \pm 10 \text{ Wm}^{-2}$, is larger than that escaping to space, $200 \pm 10 \text{ Wm}^{-2}$. About 90% of the counterradiation at the earth's surface is caused by greenhouse gases (70 %

by H₂O, 15% by CO₂, 5% by other gases), while clouds are responsible for the remaining 10%. Part of the total radiative energy input to the soil is returned to the atmosphere by infrared emission, $395 \pm 10 \text{ Wm}^{-2}$. This estimate is based on observations of outgoing surface radiation and of surface temperature averaged over the globe and over a long period of time. The emission of longwave radiation does not fully compensate for the solar flux and infrared counterradiation from the sky into the surface. The deficit of about 95 Wm^{-2} is compensated by transports of latent heat due evaporation of water at the earth's surface and condensation in the atmosphere, and sensible heat. The rate at which the release of heat due to condensation of water vapor in clouds occurs is proportional to the formation rate of precipitation multiplied by the specific heat of condensation. From observations of precipitation, which amounts about 1 m per year, it follows that averaged over the globe the latent heat transport equals $80 \pm 5 \text{ Wm}^{-2}$ [Peixoto and Oort, 1992]. The transfer of sensible heat by molecular conduction and turbulent air motions is estimated to be on average $15 \pm 7 \text{ Wm}^{-2}$ using observations and analysis by weather models [Randall *et al.*, 1992]. About $40 \pm 15 \text{ Wm}^{-2}$ of the longwave radiation, originating from the earth's surface, is directly emitted to space via the most transparent part of the spectrum, the so-called atmospheric window, without being intercepted by the atmosphere, implying an average longwave absorption of $355 \pm 15 \text{ Wm}^{-2}$ by greenhouse gases and clouds [MacCracken and Luther, 1985; Dickinson and Cicerone, 1986; Mitchell, 1989; IPCC, 1990, 1995]. From this point of view it is clear that on average the atmosphere is effectively cooled by longwave radiation, which amounts $330+200-355=175 \text{ Wm}^{-2}$.

The thermal structure of the atmosphere is determined by shortwave heating, infrared cooling as well as heating, vertical transports of sensible and latent heat and (horizontal) heat transports by dynamical processes. For the globally and annually averaged atmosphere simplifications can be made, because tendency terms due to horizontal heat advection cancel each other out. Since most of the shortwave radiation is absorbed by the earth's surface, while greenhouse gases cause a large inflow of infrared radiative energy into the surface, there is a general decrease of temperature with height in the troposphere, on average the lower 13 km of the atmosphere. In case of a purely radiative equilibrium, this vertical temperature gradient would be much larger than the dry adiabatic lapse rate, while surface temperatures would be substantially higher than observed. Latent and sensible heat flows from the surface and strong vertical mixing in the troposphere compensate for this unstable configuration of radiative equilibrium, causing an average decrease of temperature with height of 6.5 K per km. Therefore, the aforementioned convective heat flows cause a cooling of the surface and a heating of the troposphere. Also, absorption of shortwave radiation by water vapor and ozone warms the troposphere.

The radiative tendencies due to the most important atmospheric gases, active in the shortwave as well as in the longwave region, are shown in Figure 2.4. This figure is constructed by calculating the difference between the tendencies in the present atmosphere and those without the greenhouse gas under consideration, using the broad band radiative transfer scheme described in Chapter 3. Water vapor generally cools the troposphere, implying that the infrared

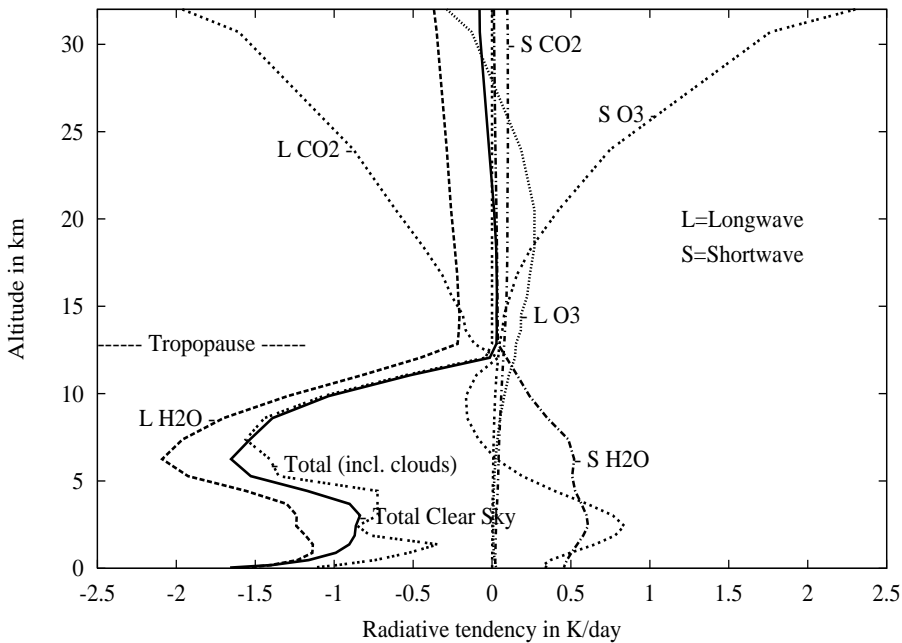


Figure 2.4: Contribution of greenhouse gases to the global mean radiative balance in terms of radiative tendencies in K/day. Also shown is the sum of these contributions in the clear sky part of the global mean atmosphere as well as including average cloudiness.

emission is larger than the absorption. CO₂ warms the lower troposphere up to about 7 km altitude. Also other greenhouse gases show a complex longwave behaviour in the troposphere, but are less pronounced than CO₂. It should be noted that there are strong radiative interactions between the various greenhouse gases [Kiehl and Ramanathan, 1982], implying that the background atmosphere influences the specific behaviour of radiative transfer by the gas under consideration (see also section 2.5). For instance, if the present mixing ratio of CO₂ is put in our model atmosphere, containing no other greenhouse gases, a longwave cooling in almost the entire troposphere shows up, which is different from what happens in reality.

The thermal structure of the stratosphere is largely determined by the absorption of solar radiation by the ozone layer, causing an increase of temperature with height. This gain of energy is balanced primarily by the strong infrared emission due to CO₂, mainly through its 15 μm band. Globally averaged, the stratosphere is in approximate radiative balance, because convection stops by definition at the tropopause, the interface between the critically unstable troposphere and the stable stratosphere. The thermal structure of the atmosphere is in turn important for the cascade of absorption and emission of infrared radiation by greenhouse gases. Emission is proportional to the Planck function (see section 2.3.3) and therefore coupled to the local

temperature. Absorption is proportional to the incident radiative flux, which is dependent on the emitted as well as the absorbed radiation upstream of the considered atmospheric level. Moreover, absorption coefficients are temperature and pressure dependent.

2.4.2 Concept of Radiative Forcing

On a global scale, perturbations of the radiation balance, either in the longwave or in the short-wave part of the spectrum, result in a climate change, since the energy balance at the top of the atmosphere has to be restored by changing the temperature of the earth's surface and the atmosphere. In reality, perturbations of the radiation balance, e.g. due to steady increases of greenhouse gases, and the subsequent climate response in terms of temperature adjustments, elapse gradually. However, the new climate equilibrium, i.e. the restored balance at the top of atmosphere, is independent of the time evolution of a radiative perturbation under the condition that the climate feedbacks behave linearly. This is at least valid for relatively small perturbations, as compared to the background radiative fluxes (see section 2.4.1). For example, doubling the CO₂ content of the atmosphere results in an imbalance of about 4 Wm^{-2} (Table 2.1), which is about 2% of the total outgoing longwave radiation at the top of atmosphere. Therefore, we may couple equilibrium climate change to instantaneous perturbations of the radiation balance. The best link between surface temperature change and radiative perturbations on a global scale is given by the net radiative flux change at the tropopause (on average at 13 km altitude) after allowing the stratospheric temperatures to adjust to a new radiative equilibrium. This net flux change at the tropopause is also known as **radiative forcing**.

The rationalization behind the concept of radiative forcing is that on global scale the stratosphere is in approximate radiative equilibrium (see section 2.4.1). Radiative adjustment is reached within a few months after applying the perturbation, whereas this adjustment takes of the order of a decade in the troposphere due to the large heat capacity of the oceans. In addition, the surface and troposphere are tightly coupled due to efficient vertical mixing processes with very short timescales and may therefore be considered as one thermodynamic (sub)system. This implies that global mean changes of the radiation at the tropopause roughly determine the final response to climate forcing mechanisms. Note that if the stratosphere reaches a new radiative equilibrium, the imbalance at the tropopause equals that at the top of atmosphere with respect to the sum of the infrared and solar radiation changes. The **climate sensitivity**, defined as the ratio of the equilibrium global mean surface temperature change to the global mean imposed radiative forcing, behaves in a near-invariant manner for both global and spatially confined forcings [Ramaswamy and Chen, 1997]. However, due to uncertainties in climate feedbacks, the climate sensitivity ranges from 0.3 to 1.1 K/Wm^{-2} among the present generation of 3D climate models [IPCC, 1995] (see section 2.6.4), mainly due to the cloud-feedback [Cess *et al.*, 1995]. This implies that an estimate of the relative climate effects can be obtained by studying the radiative perturbations [IPCC, 1997]. This issue is addressed in Chapter 5 of this thesis.

2.4.3 Climate Effects of Atmospheric Constituents

To illustrate the relative importance of atmospheric constituents, we perform numerical experiments with a 1D Radiative-Convective model, using a representative global and annual mean atmosphere in energetic equilibrium (see Chapter 5 for a description of the model as well as the input). Besides the sophisticated radiative transfer scheme, used throughout this thesis (see Chapter 3), such a model includes a convection algorithm to simulate the latent and sensible heat fluxes, which maintain a constant lapse rate in the global and annual mean atmosphere. The rationale for this approach has been described in section 2.4.2. However, we must be aware of the fact that by removing constituents with a large climate impact, the model might respond differently from the real climate system due to nonlinear processes. Nevertheless, by removing atmospheric constituents in our model, we get some insight in their relative importance. Using this model we can translate initial radiative perturbations into subsequent surface temperature responses. In Table 2.1 the temperature responses and planetary albedo changes are listed with and without water vapor feedback. The water vapor feedback has been determined by fixing the relative humidity, such that the absolute amount of water vapor varies with temperature. Some evidence has been found for such a temperature dependency of the water vapor amount, using satellite measurements of the clear sky parts of the globe, with very different surface temperatures occurring in our climate system [Raval and Ramanathan, 1989]. For values of the radiative forcing, which are smaller than about 20 Wm^{-2} in an absolute sense, our model's climate sensitivity is 0.54 K/Wm^{-2} with water vapor feedback and 0.3 K/Wm^{-2} without any feedbacks.

The constituents with the largest climate impact are related with water in all its phases. Removal of water vapor will drop the global mean surface temperature with about 20 K. Water vapor is therefore the strongest greenhouse gas, mainly due to its abundance in the atmosphere and its absorption strength per molecule. On average, liquid water and ice containing clouds cool the system ($\Delta T=5.7 \text{ K}$ without water vapor feedback). The shortwave reflection of clouds causes a radiative forcing of -49.5 Wm^{-2} , which dominates the longwave forcing of 28.3 Wm^{-2} , resulting in a net effect of -21.2 Wm^{-2} (note that for a removal of clouds, the sign of the forcing is reversed). These values of the cloud radiative forcing are in reasonable agreement with Earth Radiation Budget Experiment (ERBE) measurements, which give -48.1 Wm^{-2} and 31.0 Wm^{-2} for the shortwave and longwave spectral region, respectively [Ramanathan *et al.*, 1989]. Therefore, the warming effect of water vapor in the climate system is much stronger than the cooling effect of clouds. Hence, the net effect of removing atmospheric water vapor, liquid water, and ice is a decrease of the surface temperature by 15.6 K (Table 2.1).

Among the uniformly mixed greenhouse gases, CO_2 shows the largest effect with a radiative forcing of 23.3 Wm^{-2} , about one third of the water vapor effect. This difference is caused by the fact that on average the column amount of water vapor ($\approx 20 \text{ Kg m}^{-2}$) is about four times larger than the CO_2 column amount, while H_2O is also a stronger absorber and emitter than

Table 2.1: Radiative forcing in Wm^{-2} and climate impact in terms of surface temperature change, ΔT in K, as well as planetary albedo change, $\Delta\alpha_p$ in %, due to the removal of several atmospheric constituents as calculated by the KNMI Radiative-Convective Model (KRCM, see Chapter 5). Global average surface albedo remains unchanged in these numerical experiments. For cases where water vapor is removed from the model atmosphere, its feedback calculations make no sense (denoted by *).

Atmospheric composition	Radiative Forcing in Wm^{-2}	Without H ₂ O feedback		With H ₂ O feedback	
		ΔT in K	$\Delta\alpha_p$ in %	ΔT in K	$\Delta\alpha_p$ in %
double CO ₂ mixing ratio	+4.0	+1.2	-0.1	+2.2	-0.2
removal CO ₂	-23.3	-6.8	+0.4	-12.0	+1.3
removal CH ₄	-1.5	-0.5	+0.0	-0.9	+0.1
removal N ₂ O	-1.2	-0.4	+0.0	-0.7	+0.1
removal CFCs	-0.3	-0.1	+0.0	-0.2	+0.0
removal background aerosols	+2.6	+0.8	-0.8	+1.5	-0.9
removal O ₃	-3.5	-1.1	+2.0	-2.0	+2.2
removal water vapor	-66.2	-20.4	+4.0	*	*
removal clouds	+21.2	+5.7	-14.2	+12.8	-14.7
removal water vapor and clouds	-62.5	-15.6	-12.0	*	*
atmosphere containing N ₂ only	-111.9	-23.0	-12.8	*	*

CO₂ per molecule (see Chapter 3). On the other hand, most of the water vapor is situated in the lower atmosphere, whereas CO₂ is uniformly mixed. In terms of radiative forcing and climate effect, infrared radiatively active molecules are more effective if they are located in atmospheric regions with a large temperature contrast with respect to the surface [Lacis *et al.*, 1990; Van Dorland and Fortuin, 1994; Chapter 4].

The effect of doubling the CO₂ mixing ratio has much less effect than removing this gas from the atmosphere due to the logarithmic behaviour of the relationship between forcing and mixing ratio at present levels [IPCC, 1994; 1995]. In case of the new equilibrium for an atmosphere containing the double amount of CO₂ and more water vapor due to the feedback, the radiation balance at the top of atmosphere is restored, with somewhat less reflected shortwave radiation (see albedo change in Table 2.1) and thus more outgoing longwave radiation. The largest flux changes occur at the surface in the longwave component: the upward longwave radiation increases with 11.9 Wm^{-2} in agreement with the increase in surface temperature. Since atmospheric temperatures are tightly connected with that of the surface and due to the increase of opacity, the longwave counterradiation increases somewhat more with 14.1 Wm^{-2} (compare with Figure 2.3). The increase of the absorption of solar radiation by H₂O and CO₂ causes a decrease of absorbed radiation by the surface of about 1.9 Wm^{-2} , while the latent and sensible heat flows are slightly increased (0.3 Wm^{-2}). These values imply that the atmospheric shortwave heating increases (2.7 Wm^{-2}), and that the atmosphere is more efficiently cooled by longwave radiation (3.0 Wm^{-2}). This paradox of increased atmospheric longwave cooling in

a warmer double CO₂ climate is quite similar to the effect of net atmospheric cooling for the natural greenhouse effect (Figure 2.3 and section 2.4.1). In the latter case the cooling per degree is approximately $175/33=5.3 \text{ Wm}^{-2}/\text{K}$. This is about four times larger than the additional longwave cooling in case of doubling the CO₂ content (see Table 2.1) due to the logarithmic relationship between the present amount of water vapor as well as CO₂ and their climate effects.

Removing O₃ from the atmosphere destroys the temperature structure of the stratosphere due to the strong reduction of shortwave absorption [Van Dorland and Fortuin, 1994; Shine *et al.*, 1995]. Its consequence is that convective heat flows penetrate to higher altitudes in the atmosphere, resulting in a lift of the tropopause level. This is likely to cause additional climate effects, which cannot be derived from the value of the radiative forcing, computed here as the change in net flux at a fixed tropopause level (at 179 hPa in the equilibrium atmosphere) after adjustment of the stratospheric temperatures.

The last case in Table 2.1 represents an atmosphere from which all absorbing constituents are removed, while only Rayleigh scattering (e.g. 100% N₂ atmosphere) is permitted. In such an atmosphere the surface temperature will be about 23 K lower than the present value. The discrepancy with the estimate of the natural greenhouse effect, about 33 K (Chapter 1), is caused by the fact that the planetary albedo is different, mainly due to the absence of clouds.

2.5 Analysis of the greenhouse effect

2.5.1 Simple Analytical Model for Longwave Radiative Transfer Characteristics

Longwave radiative transfer in the atmosphere is governed by sources (thermal emission) and sinks (absorption) of radiant energy (section 2.3.3). The longwave absorption coefficient shows a variation with frequency by several orders of magnitude. The absorbed radiation is proportional to the incident flux, while the absorptivity, i.e. the ratio between the absorbed and incident radiation, is dependent on temperature, pressure, and the amount of greenhouse gases, all varying with altitude in the atmosphere. As explained in section 2.3.2, the emission of infrared radiation is dependent on the emissivity, which is equal to the absorptivity according to Kirchhoff's law. In contrast to absorption, emission is proportional to the Planck function (Eq.2.1). Thus, the temperature structure of the atmosphere is important for the emission process. These different dependencies of the sources and sinks result in a rather complex infrared atmospheric radiative transfer process. Therefore, numerical methods are essential for achieving sufficient accuracy of the infrared radiative fluxes.

Nevertheless, some qualitative insight in infrared radiative transfer can be obtained by making the proper simplifications of the governing equation (Eq.2.4). In this section (2.5.1) we aim to present our analytical model for longwave radiative transfer restricted to the troposphere. In section 2.5.2 we discuss the enhanced greenhouse effect in terms of flux changes due to a step increase of greenhouse gases, which is usually done for the determination of the radiative forcing (see also Chapter 4). In section 2.5.3 the altitude at which radiation is effectively emitted

and its change are considered in order to get a complete overview on the mechanism of the greenhouse effect.

We limit ourselves to the troposphere for three reasons: firstly, the troposphere contains about 80% of the total atmospheric mass, determining largely upward radiative transfer throughout the atmosphere and also the downward component in the lower troposphere at least in most parts of the spectrum. Therefore, we put emphasis on the upward flux and its change. Secondly, flux changes at the top of this layer determine the radiative forcing (section 2.4.2). Although the radiative forcing due to increases of greenhouse gases is partly determined by the increase of the downward flux through enhanced emission from the stratosphere, the contribution from the change in upward flux is much more complex due to the higher density of greenhouse gases in the troposphere. Moreover, the mechanism of the upward flux change due to increases of greenhouse gases is sometimes misinterpreted, e.g. *Barrett [1995]* (and discussed by *Van Dorland [1995]*). Thirdly, globally and annually averaged, the temperature in the troposphere decreases with altitude (section 2.4.1) and so does the Planck function in all spectral regions (section 2.3.2). This property is used in our analytical approach.

Assuming a horizontally homogeneous atmosphere, the broad-band upward (F^+) and downward fluxes (F^-) at altitude z , which are found by angular integration of Eq.2.4 over the two half-spheres and integration over broad band spectral intervals, can then be written as (e.g. *Stephens [1984]*, but applied to the troposphere):

$$F^+(z) = B_s \tau(z, 0) + \int_0^z B(z') \frac{d\tau(z, z')}{dz'} dz', \quad (2.5)$$

and

$$F^-(z) = F_t^- \tau(z_t, z) - \int_z^{z_t} B(z') \frac{d\tau(z', z)}{dz'} dz', \quad (2.6)$$

where F_t^- is the downward flux at the tropopause due to stratospheric emission, z_t is the height of the model's top, and τ is the (diffuse) transmission function between z and z' , defined as $\tau(z, z') = \exp(-k(z - z'))$ for upward radiation ($0 \leq z' \leq z$) and $\tau(z', z) = \exp(-k(z' - z))$ for downward radiation ($z \leq z' \leq z_t$). Strictly speaking, these quantities are monochromatic, but for our purpose extended to broad band intervals, keeping the characteristic behaviour of atmospheric transmission. Here, k is defined as the absorption coefficient per unit of distance. Both upward and downward fluxes (Eq.2.5 and Eq.2.6) are defined positive. The upward flux can be separated in an attenuated terrestrial flux, F_{ter}^+ , and an atmospheric flux, F_{atm}^+ (first and second term at the RHS of Eq.2.5, respectively). Similarly, the downward flux is separated into an attenuated stratospheric flux and a tropospheric flux, both originating from the atmosphere itself (Eq.2.6).

By further simplifications of Eq.2.5 and Eq.2.6, a set of three parameters appears to be sufficient to understand the essence of radiative transfer and the changes therein due to perturbations of greenhouse gas mixing ratios. These three parameters are: (1) the Planckfunction at the surface, B_s , and tropopause, B_t , for the upward and downward component of the radiative flux,

respectively, (2) the change of the Planck function with some measure for altitude, $\Gamma = -\partial B/\partial z$ (referred to as Planck lapse rate), and (3) the absorption coefficient, k . As a first order approximation, we assume the parameters Γ and k to be constant with respect to z . The constancy of Γ implies that the Planck function at altitude z can be written as: $B(z) = B_s - \Gamma z$. The constancy of k implies that z cannot be equal to the geometrical height, since the effective amount of long-wave absorbers decreases even faster than pressure in the atmosphere, due to the water vapor distribution and to temperature and pressure dependences of the absorption coefficient (see section 2.3.3). Hence, the z -coordinate increases more rapidly in the lower troposphere than higher up as compared to the geometrical altitude. Therefore, only qualitative statements can be made using this approach. However, the characteristics of the radiative fluxes and their changes due to increases of greenhouse gases, calculated with this analytical model, are compared with those of a sophisticated radiative transfer scheme using a clear sky atmosphere. This is done to avoid steep changes in the absorption coefficient in the vicinity of clouds, which can be considered as black bodies for longwave radiation even for small values of the liquid or ice water paths.

Our approximations yield for the upward fluxes (using Eq.2.5):

$$F_{ter}^+(z) = B_s \exp(-kz), \quad (2.7)$$

and

$$F_{atm}^+(z) = [B_s + \frac{\Gamma}{k}][1 - \exp(-kz)] - \Gamma z. \quad (2.8)$$

Hence, the total upward flux can be written as:

$$F^+(z) = B_s - \Gamma z + \frac{\Gamma}{k}[1 - \exp(-kz)]. \quad (2.9)$$

For the downward flux below the tropopause we find (using Eq.2.6):

$$F^-(z) = F_{atm}^-(z) = F_t^- \exp(-k(z_t - z)) + [B_t - \frac{\Gamma}{k}][1 - \exp(-k(z_t - z))] + \Gamma(z_t - z). \quad (2.10)$$

To illustrate the validity of our approximations in the tropospheric radiative transfer equation, we discuss the characteristics of the (components of) the upward flux by making a comparison with calculations performed with the sophisticated radiative transfer model, shown in Figure 2.5. The upward terrestrial flux decreases with height due to absorption by greenhouse gases. At the top of the atmosphere this flux amounts 75 Wm^{-2} , which is about twice the value in a global mean atmosphere including clouds (section 2.4.1). In the atmospheric window region (8-12.5 μm) this decrease is considerably less than outside this region.

The upward atmospheric flux starts at zero just above the surface by definition and reaches a maximum at height $z_{max} = k^{-1} \ln(1 + B_s k/\Gamma)$, which is obtained from the vertical derivative of Eq.2.8. This implies that below this maximum, emission is larger than absorption, while above this level the atmospheric flux is large enough to establish more absorption than emission. This is reinforced by the fact that emission decreases with height due to the Planck lapse rate.

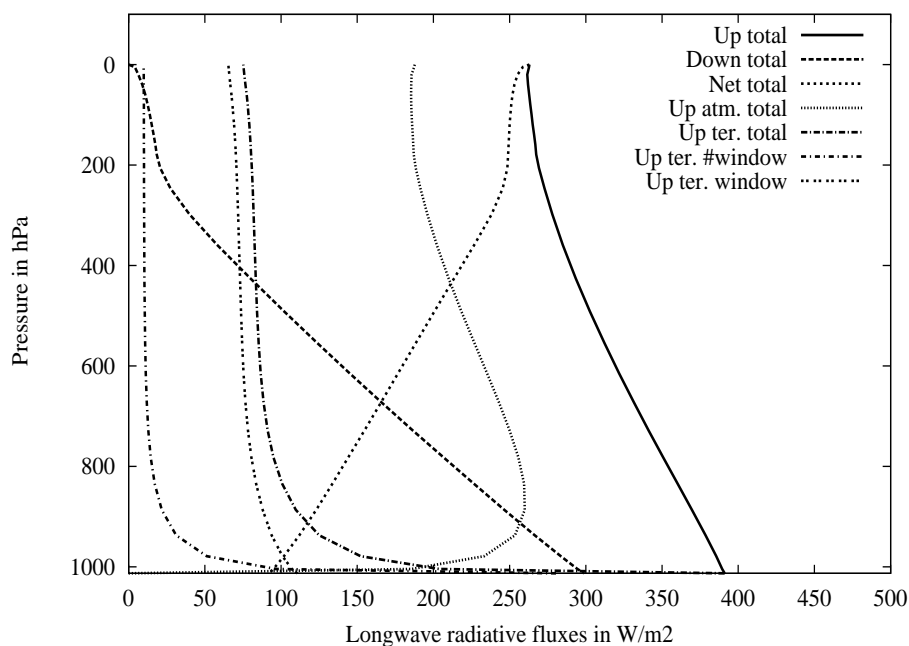


Figure 2.5: Longwave characteristics of the clear sky part of the global mean atmosphere as computed using a broad band radiative transfer scheme. The curves shown are the total (spectrally integrated) upward, downward and net fluxes. The total upward flux is splitted into the terrestrial and atmospheric fluxes. The terrestrial (upward) flux is also shown for the atmospheric window region (8-12.5 μm) and for the remainder of the spectrum (indicated by #window).

In transparent parts of the spectrum the atmospheric flux becomes very small and z_{max} approximates the scale height B_s/Γ , which is of the order of the tropopause height, but dependent on the chosen spectral interval. The annual mean global atmosphere has $z_{max} \approx 1340$ m in the absence of clouds, which is obtained from the radiation calculation (Figure 2.5). Using typical spectrally integrated values of B_s (395 Wm^{-2}) and Γ (0.02 Wm^{-3}), the absorption coefficient equals the value $k \approx (330 \text{ m})^{-1}$, and can be considered as the inverse of the average penetration depth for longwave radiation in the atmosphere close to the surface (note that this result is quite insensitive to variations of Γ). Thus spectrally averaged, the atmosphere contains about one optical depth of absorbing matter between the surface and about 330 m.

The total upward flux (Eq.2.9) decreases with height in the troposphere and this decrease is proportional to the Planck lapse rate, Γ , and the absorptivity, $(1 - \exp(-kz))$, as can be calculated from the vertical derivative of the total flux. Therefore, the decrease of the upward flux with height is larger for opaque atmospheres as compared to transparent atmospheres. In the opaque limit the flux change equals the Planck lapse rate, implying that the total upward flux

consists completely of the emitted radiation at the considered atmospheric level. This can also be derived from Eq.2.9 for large values of k .

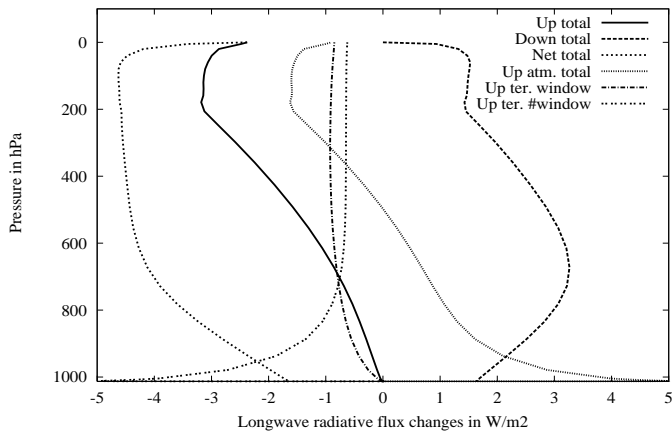
2.5.2 Enhanced Greenhouse Effect

Instantaneous increases of greenhouse gases result in changes of longwave radiative fluxes throughout the atmosphere. But due to the fact that their absorption bands are located in different parts of the spectrum, doubling the CO₂ content of the atmosphere results in quite different radiative profile changes as compared to doubling the content of chlorofluorocarbons (CFCs), as shown in Figure 2.6a and 2.6b, respectively. The most important CFC absorption bands are situated in the atmospheric window, whereas CO₂ has its strongest absorption band in the 15 μm region outside this window. Using the analytical model described in the previous section, we are able to show the most important features leading to these differences. Instantaneous concentration changes can be simulated by taking the derivative of the upward and downward longwave fluxes with respect to the absorption coefficient. The change in the total upward flux can thus be written as:

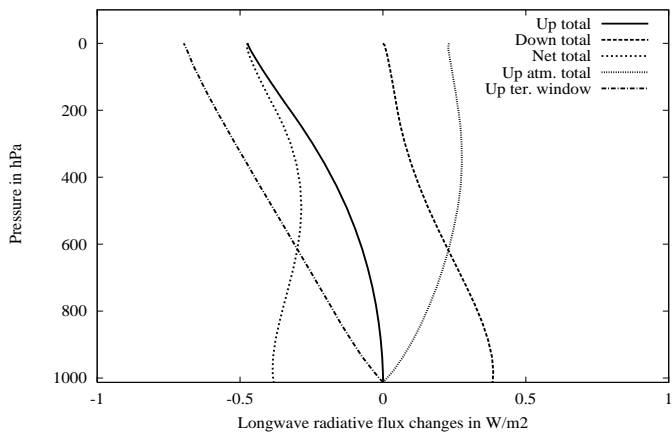
$$\frac{dF^+(z)}{dk} = -\frac{\Gamma}{k^2}[1 - (1 + kz)\exp(-kz)] \quad (2.11)$$

Therefore, the upward flux is always reduced for decreasing temperatures with height (positive Γ), except at the surface where the flux difference is zero by definition due to an initially unchanged surface temperature. Most pronounced is the fact that the approximated flux reduction is not dependent on B_s (Eq.2.11). In the transparent limit $k \ll 1$ the flux change is a parabolic function of the vertical coordinate used: $\Delta F^+(z) = -\Gamma z^2 \Delta k / 2$, while in the opaque limit $k \gg 1$ the flux change is given by: $\Delta F^+(z) = -\Gamma \Delta k / k^2$, which becomes very small for large values of k . This is known as saturation.

The characteristics of the flux changes can be illustrated by comparing extreme values, derived from the analytical model, with the radiation calculations, shown in Figure 2.6a and 2.6b. For an increase of greenhouse gases and thus of atmospheric opacity (denoted by subscript dk), the largest terrestrial flux reduction occurs at height $z_{ter,dk} = k^{-1}$, while the maximum increase of the atmospheric flux takes place at a lower level $z_{atm,dk} = [k + \Gamma/B_s]^{-1}$. The opacity of the atmosphere in the vicinity of the 15 μm band of CO₂ results in almost the same extreme values reached at an altitude of about 9 m ($z_{atm,dk} \approx z_{ter,dk}$) for a doubling of CO₂ (just above the surface in Figure 2.6a). Terrestrial flux changes in the window region due to weaker CO₂ bands show an extreme value at about 9 km (Figure 2.6a). For a doubling of the CFCs the maximum of the atmospheric flux change is located at about 9 km (Figure 2.6b), while no minimum in the terrestrial flux changes is found in the troposphere (at some distance above the tropopause the parameter Γ changes sign). Differences of the computed penetration depths in the window region derived from the terrestrial flux change between the doubling CO₂ and CFCs cases are caused by the fact that the weak CO₂ bands in the window region show a much larger temperature dependency than the CFC bands, which is not taken into account in our approximation.



(a)



(b)

Figure 2.6: Longwave flux changes in the clear sky part of the global mean atmosphere due to a doubling of CO_2 (a) and CFCs (b) as computed using a broad band radiative transfer scheme. The curves shown are the total (spectrally integrated) upward, downward and net fluxes. The total upward flux is splitted into the atmospheric flux and the terrestrial flux for the atmospheric window region ($8\text{-}12.5\mu\text{m}$) and for the remainder of the spectrum (indicated by #window). For increases of CFCs the latter is approximately zero.

The radiative forcing due to increases of greenhouse gases can be separated into the contributions of the change in downward flux, upward terrestrial flux and the upward atmospheric flux at the tropopause. The former has not been accounted for in our analytical model, but radiation calculations indicate that the downward flux always increases due to enhanced emission from the stratosphere, resulting in a positive contribution to the radiative forcing (Figure 2.6a

and 2.6b). Due to the enhancement of atmospheric absorption a larger fraction of upward terrestrial radiation, originating from the surface, is captured and reduces the longwave radiation at all levels in the atmosphere, resulting in a positive radiative forcing, i.e. flux reduction at the tropopause. This part of the radiative forcing is independent of the Planck lapse rate in the troposphere. Simultaneously, the emission and absorption of radiation, originating from atmospheric layers, is increased. If a greenhouse gas is absorbing and emitting in the atmospheric window region (e.g. CFCs), the increase in emission dominates the increase in absorption, counteracting the radiative forcing due to the change in terrestrial flux at the tropopause level (Figure 2.6b). If a greenhouse gas is mainly absorbing and emitting in the opaque part of the spectrum the increase in absorption dominates the increase in emission above a certain level (about 500 hPa for CO₂), resulting in negative values of the flux change (Figure 2.6a). For CO₂ the reduction of the terrestrial and the atmospheric fluxes at tropopause level, if spectrally integrated, contribute equally to the radiative forcing. However, the reduction of the terrestrial flux is mainly caused by the weaker bands of CO₂ in the window region showing a similar behaviour as for increasing the amount of CFCs. In all cases the sum of the radiative forcings of the changes in terrestrial and atmospheric flux changes is positive for increases of greenhouse gas concentrations as stated by Eq.2.11. Hence, the net upward longwave radiation is reduced by a smaller upward as well as a larger downward flux, both contributing to a positive radiative forcing. It should be emphasized that we approximate the radiative forcing by using the fixed temperature concept, i.e. without the temperature adjustment of the stratosphere (see definition in section 2.4.2). In case of doubling CO₂ the global average stratosphere cools above the 100 hPa level, resulting in a smaller increase of the downward flux at the tropopause. However, this does not affect our qualitative results. We may conclude that for greenhouse gases active in the window region the radiative forcing due to upward flux changes originates mainly from the terrestrial flux reduction, whereas for gases active outside the window region the reduction of the atmospheric flux contributes most to the radiative forcing.

The importance of the Planck lapse rate for the greenhouse effect can be illustrated by considering an isothermal atmosphere, with the surface held at the same temperature. In such an atmosphere the total upward flux is constant with height and equals B_s . This is due to the fact that the absorbed radiation is also emitted at the same temperature (Eq.2.5). In addition, the downward flux at the surface equals the upward flux at the top of atmosphere. The tropopause, defined as the level at which a temperature minimum occurs, does not exist and should be placed at the top of atmosphere. In such a hypothetical atmosphere, there is no radiative forcing, i.e. no change of net flux at the top of atmosphere due to changing concentrations of greenhouse gases. Throughout the atmosphere, there is no change in upward flux as can be deduced from Eq.2.11 with $\Gamma = 0$, while the downward flux is zero at the top of atmosphere by definition and so is its change. This illustrates that the greenhouse effect of infrared radiatively active gases is tightly coupled to the tropospheric Planck lapse rate, and therefore to the general decrease of temperature with altitude.

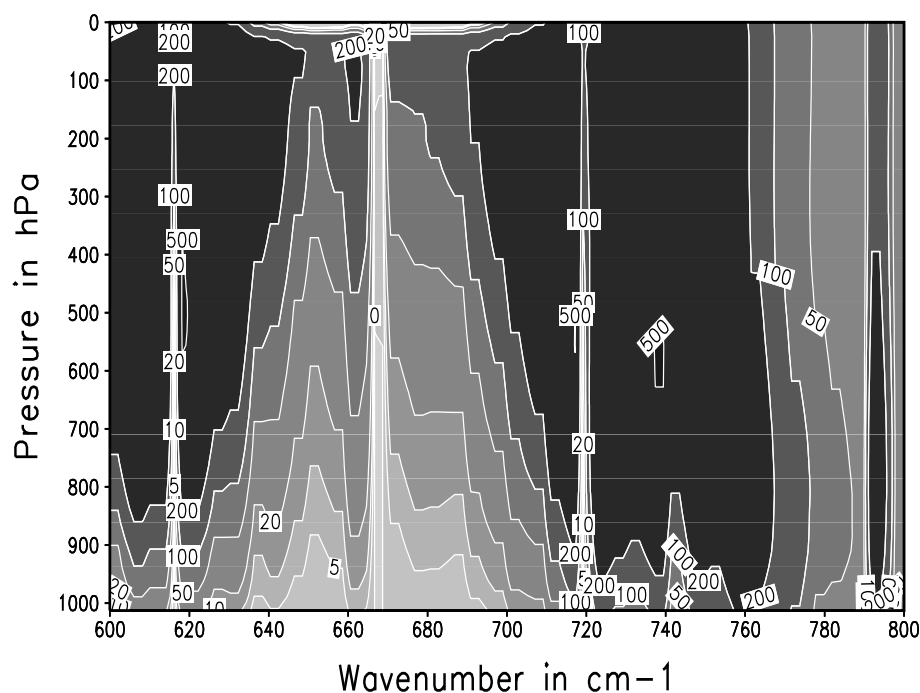


Figure 2.7: Change of net spectral flux (downward minus upward) in $\text{Wm}^{-2}/\mu\text{m}^{-1}$ in the $15 \mu\text{m}$ ($= 667 \text{ cm}^{-1}$) region due to a doubling of the CO_2 concentration as calculated with a narrow band radiative transfer scheme based on the Morcrette and Fouquart [1985] scheme.

Finally, we discuss the absorption bands of CO_2 to illustrate their contribution to the enhanced greenhouse effect. Figure 2.7 shows the change of the net spectral flux due to a doubling of CO_2 calculated with a narrow band radiative transfer scheme. At the tropopause, situated at 179 hPa, the integrated net spectral flux equals the instantaneous radiative forcing. In the center of the $15 \mu\text{m}$ region the net flux change is approximately zero in the troposphere and the lower stratosphere due to the opacity of the atmosphere, which is called saturation. Although we derived this opaque limit for the change in upward radiation only (Eq.2.11), it is equally valid for downward radiation, but with opposite sign. The so-called wings of the $15 \mu\text{m}$ band, consisting of overlapping rotational lines, absorb less strongly so that there is no saturation here. The $12.5\text{-}20 \mu\text{m}$ region contributes with about 90% to the total radiative forcing due to CO_2 changes [Van Dorland, 1995]. The remaining 10% of the total forcing takes place in the window region ($8\text{-}12.5 \mu\text{m}$) due to various weaker bands of CO_2 . This clearly demonstrates the importance of the wings of the $15 \mu\text{m}$ CO_2 band in the global warming problem.

2.5.3 Analysis in Terms of Effective Temperature

Infrared fluxes in clear sky atmospheres show large variations with respect to frequency due to the presence of greenhouse gases. The only exception is the upward flux just above the earth's surface, which closely resembles a black body, resulting in an almost perfect Planck curve at the local surface temperature (section 2.3.2). In fact, the spectral signature of atmospheric gases in the radiation fluxes, which is a measurable quantity, is a proof of the thermal emission by the atmosphere and hence a confirmation of our understanding of the interactions between infrared radiation and greenhouse gases.

Fluxes can be expressed in terms of effective temperature, i.e. the temperature of a black body emitting the same flux in a certain spectral region. If applied to the total spectrum, the effective temperature can be computed by equating the Stefan-Boltzmann law to the total flux: $F = \sigma T_{eff}^4$. The spectral effective temperature is a measure of the altitude at which infrared radiation in a particular spectral region is effectively emitted. Using Eq.2.10 for downward radiation, we find for the effective radiative altitude, defined as the altitude at which the atmospheric temperature equals the effective temperature, neglecting the radiative contribution from the stratosphere: $z_{eff} = k^{-1}(1 - \exp(-kz_t))$. If the absorption coefficient k is not too small, then $z_{eff} \approx k^{-1}$ i.e. if the effective altitude is much lower than the tropopause. This implies that the effective altitude is a measure of the (inverse) absorption coefficient or average pathlength at which emitted radiation is absorbed. Thus the atmosphere contains about one optical depth of absorbing matter for infrared radiation between the surface and this effective altitude.

We apply the concept of effective temperature to a typical clear sky mid-latitude summer atmosphere with a surface temperature of 294 K. Radiative fluxes at the surface and at the top of the atmosphere are calculated with a sophisticated narrow band radiative transfer scheme (see Chapter 3) and converted into effective temperatures for each of the 225 spectral intervals, which are shown in Figure 2.8. The effective temperatures for downward radiation in the 5-8 μm region and for wavelengths larger than 12.5 μm are approximately equal to the surface temperature, indicating a large opacity of the atmosphere due to water vapor and CO_2 . In the vicinity of the strong 15 μm band of CO_2 , an average pathlength of the order of 1 cm is found. In the atmospheric window, between 8 and 12.5 μm , the atmosphere is much more transparent. In this region the effective temperature is about 250 K, corresponding to average pathlengths of the order of 7 km. This is somewhat smaller than in our previous analysis (section 2.5.2), due to the fact that in this spectral region the atmosphere is sufficiently transparent to lower the effective altitude as compared to the inverse absorption coefficient (k^{-1}). In the vicinity of the 9.6 μm band, the average pathlength is somewhat smaller as compared to the remaining part of the atmospheric window region due to the presence of ozone in the atmosphere.

The outgoing longwave radiation at the top of the atmosphere (Figure 2.8) shows much more structure than the downward radiation at the surface due to the fact that water vapor is concentrated in the lower atmosphere. Therefore, the infrared signature of other greenhouse

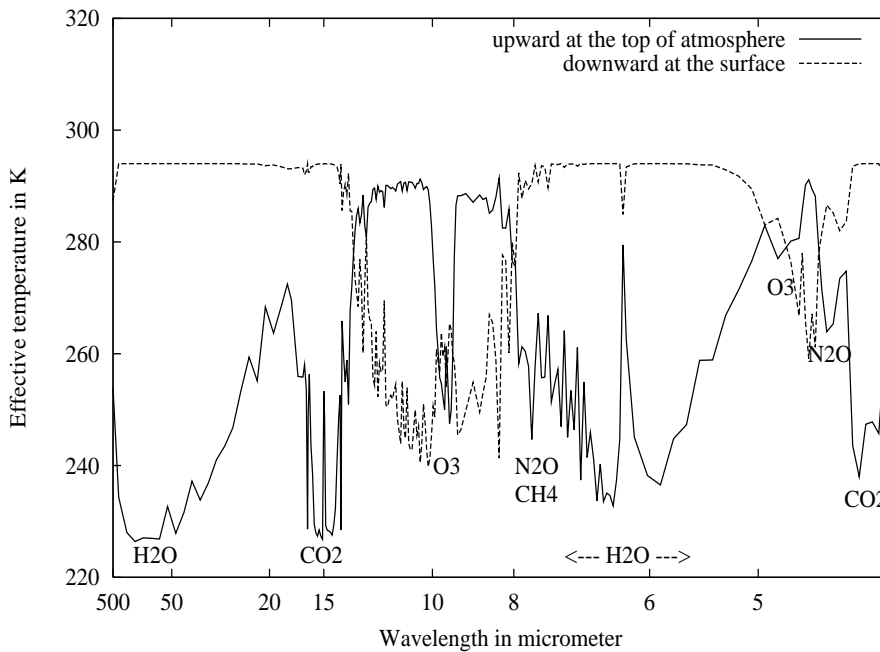


Figure 2.8: Effective temperature (in K) of longwave radiation as function of wavelength (in μm) in a reference clear sky Mid-Latitude Summer atmosphere with a surface temperature of 294 K for upward radiation at the top of atmosphere and downward radiation at the surface.

gases such as CO_2 and O_3 is much more pronounced at the top of the atmosphere. Using the analytical model, described in section 2.5.1, we find an analogous definition for the effective altitude of upward radiation at the top of the atmosphere as for downward radiation at the surface, namely the tropopause height minus this effective altitude (for the downward flux). However, if the atmosphere is almost black, i.e. in the center of the 15 μm band of CO_2 , radiation is effectively emitted from a stratospheric level (at 230 K in Figure 2.8), breaking down our simple relationship. On the other hand, if the atmosphere is quite transparent, i.e. in large parts of the atmospheric window, a significant fraction of the outgoing longwave radiation originates from the earth's surface, such that the effective altitude is close to the surface (Figure 2.8).

Increases of all greenhouse gases, no matter in which part of the spectrum they are radiatively active, lead to an increased opacity (except in the saturated parts of the spectrum) and therefore result in a reduction of the net upward longwave flux at the tropopause, which is identical to a positive radiative forcing. This reduction consists of a decrease in upward radiation (Eq.2.11) and an increase in downward radiation. Figure 2.9 shows the radiative effect of a doubling the CO_2 mixing ratio in terms of change in effective temperature. The downward radiation at the earth's surface is increased everywhere at the wavelengths where CO_2 is radiatively active. This

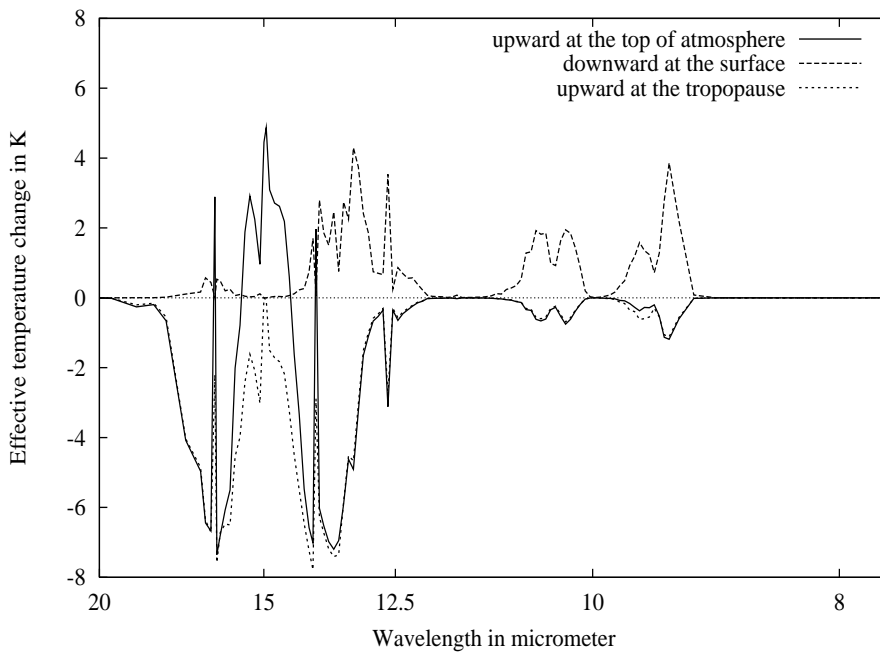


Figure 2.9: Change of effective temperature (in K) as a function of wavelength (in μm) in a reference clear sky Mid-Latitude Summer atmosphere due to a doubling of the CO_2 concentration for downward radiation at the surface and upward radiation at the top of the atmosphere and tropopause, respectively.

can be interpreted as radiation which is effectively emitted from a lower atmospheric level. In the vicinity of the center of the $15 \mu\text{m}$ band, the increase is practically zero due to saturation. Also, in the same spectral region the outgoing longwave radiation at the top of the atmosphere is increased due to the fact that the effective altitude of emission is located in the stratosphere where the temperature increases with height. In spectral regions with effective emission altitudes in the troposphere, the effective temperature decreases, implying that these altitudes increase. The upward longwave radiation at the tropopause is reduced everywhere, in agreement with Eq.2.11, while no change is found at the center of the saturated $15 \mu\text{m}$ band of CO_2 . This reduction can thus be interpreted as an increase in the effective altitude in the troposphere, where temperatures are lower. This again demonstrates that the Planck lapse rate (Γ) as a consequence of the natural atmospheric content of the radiatively active constituents plays an essential role in the enhanced greenhouse effect.

It should be emphasized that the increased counterradiation, changing the surface balance, is not the basic reason for the enhanced greenhouse effect. It is the imbalance at the tropopause (the so-called radiative forcing), which equals the imbalance at the top of atmosphere after a relatively fast stratospheric temperature adjustment towards a new radiative equilibrium, which

forces global climate to change. This change requires some time, of the order of a decade, due to the large heat capacity of the world's oceans (see section 2.6.4). The disturbed balance of less outgoing infrared radiation as compared to the net incoming solar radiation can only be restored by an increase of the temperature at the earth's surface and in the troposphere, such that eventually at the higher emission altitude the temperature reaches approximately the same value as at the (lower) effective altitude in the unperturbed state.

2.6 The Science of Climate Change

2.6.1 Climate Issues

The science of climate change tries to find answers on two main issues. The first issue is the detection of climate change from instrumental records. Observations with the highest confidence level in combination with the longest time series are temperature data (Figure 2.10), e.g. in contrast with precipitation data. An important question is how exceptional the observed warming trends and fluctuations are during this century as compared to those in the pre-industrial era. In order to answer this question, knowledge is needed on the amplitude of the natural variability of the climate system, occurring on a variety of space and time scales. We may distinguish internally and externally driven variability. Internal variability is caused by interactions between atmosphere, oceans, cryosphere and biosphere, hence between the components of the climate system. The climate can be externally driven by changes in solar activity or due to the volcanic aerosol content of the atmosphere (assuming no causality between climate state and volcanic eruptions).

At this stage of research, large uncertainties remain in the estimates of the natural variability. This points towards the second main issue, namely the attribution of causes of climate change. The attribution issue concerns the ability to separate the signal of human effects, roughly the enhanced greenhouse effect due to increases of anthropogenic trace gases minus the cooling effects of manmade aerosols, from the natural variability. Attribution is difficult because of uncertainties in the histories and magnitudes of natural and anthropogenic forcings. In addition, it is likely that we have not perceived all mechanisms leading to natural variability. Nevertheless, the limited available evidence from proxy climate indicators suggests that the 20th century global mean temperature is at least as warm as any other century since at least 1400 AD [IPCC, 1995].

Another approach to the attribution problem is the comparison of observed regional patterns of temperature changes with 3D climate model results, using various sets of possible scenarios for the human influence. *Santer et al.* [1996] found that using the changes of both the greenhouse gases (parameterized as CO₂ equivalents) and sulfate aerosols since preindustrial times, a much better agreement is reached with the observed changes of near-surface air temperature patterns than for the "CO₂-only" scenario. The cautious conclusion may be drawn that the probability is quite low that these correspondences could occur as a result of natural internal variability

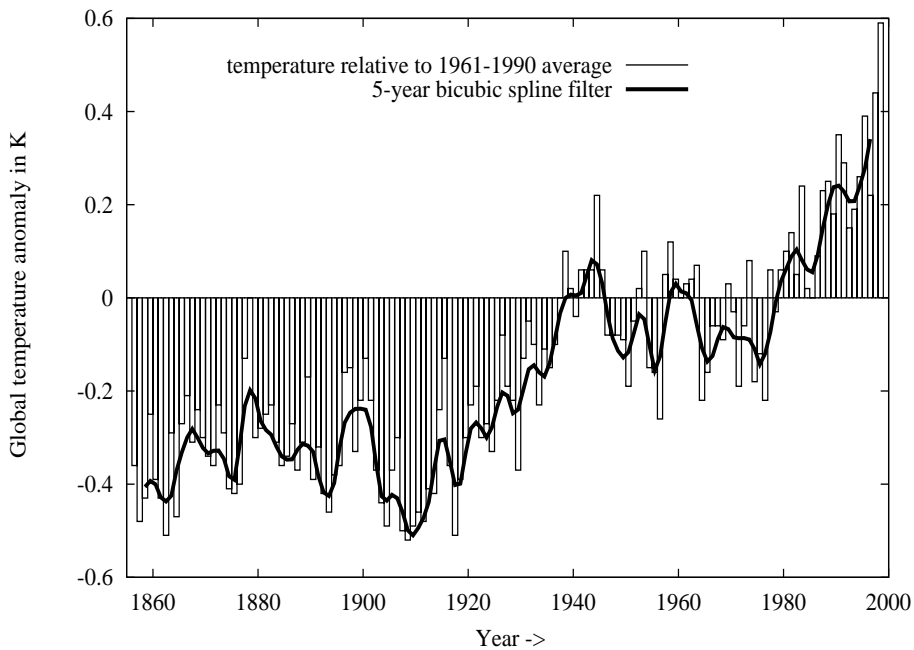


Figure 2.10: Observed global mean near surface air temperature trend since 1856 relative to the climatological average 1961-1990 [Jones, 1994, updated to 1998]: the solid curve represents smoothing of the annual mean values shown by the bars to suppress interannual variability.

only. However, through the impact of external forcing mechanisms with possible variations on decadal time scales, unequivocal proof of a human influence on climate cannot be given.

2.6.2 Climate Change

All through the geologic past and human history climate and atmospheric composition have been changing. Changes occur at practically all time scales from years to thousands of years. A well known example of the latter is the occurrence of ice ages. During the last one, which had its maximum some 18,000 years ago, global average temperature most probably was 3-4 K lower than at present, while the CO_2 concentration of the air amounted to only 60% of the present value [IPCC, 1990]. There are strong indications that the alternation of ice-ages and interglacials are triggered by periodic changes of earth's orbital parameters, namely the precession of the equinoxes, the axial precession and the precession of the ellipse, on timescales of 20,000 to 100,000 years. These are the so-called Milankovitch orbital effects. After the last ice age global temperatures reached present levels at about 12,000 years before present. Since then variations were numerous but their amplitude has generally been smaller than 2 K on a world average

basis. From this point of view it is clear that climate changes as shown in Figure 2.10 are not necessarily related to some anthropogenic cause.

The changes we observe at present in earth's climate show a general tendency for warming, i.e. an increase of the global average near surface air temperature of about 0.4-0.7 K over the past century (Figure 2.10) and a retreat of mountain glaciers all over the world [IPCC, 1990]. Related to this, a sea level rise of approximately 15 cm over the past century is observed. Climate changes of this extent, however, are not an unusual phenomenon. Regional changes of climate are larger and even more common than changes in a global average sense. In fact, it may happen that climate is changing almost everywhere without a net global average change of e.g. temperature and precipitation. Alternatively, changes of global average temperature may be very unequally distributed over the globe. This means that regional changes of climate are far less predictable than global average changes [Schuurmans, 1988]. The central question in climate research is how much of the warming trend in the observed global mean temperature (Figure 2.10) can be attributed to the human influence.

Over ages, human communities have had little or no effect on the composition of the global atmosphere. In the last one-and-a-half century the rapid growth of the world's population and the development of technology caused an immense increase of energy use. Most of this energy was and still is produced by burning fossil fuels. The direct consequence has been an increase of the atmospheric CO₂ level by about 30% since 1850, the beginning of the industrial era. Routine measurements of the concentration of atmospheric CO₂, which started in 1958, clearly show an average increase of about 0.4% per year [IPCC, 1995]. The CO₂ concentration has reached a level of 365 ppmv (parts per million by volume) in 1998. Isotopic analysis suggests that this increase is largely due to human activity. Anthropogenic emissions of CO₂ are partly absorbed by the oceans (35-40%) and the biosphere (5-10%). The remanent fraction of CO₂ in the atmosphere, at present 50-60%, is dependent on temperature and biotic content of the oceans as well as on the changes in the amount and type of vegetation. The concentrations of other naturally occurring greenhouse gases, such as CH₄ and N₂O, are increasing rapidly by human activities such as the combustion of fossil fuels, urbanization, agriculture and deforestation. Also the level of purely anthropogenic trace gases, like chlorofluorocarbons (CFCs), has increased. Besides the fact that CFCs are strong greenhouse gases, they chemically destroy the ozone layer in the upper atmosphere. It is due to the latter effect that international agreements have been made on a production stop. Since 1992, increases of CFC-concentrations are slowing down. The radiative forcing due to changes of the aforementioned well-mixed greenhouse gases is known within the relatively small uncertainty limit of about 15%. CO₂ contributes most to this forcing with about 60%.

In addition to these uniformly mixed greenhouse gases, various short-lived radiatively active atmospheric constituents have changed due to industrial activities. Emissions of NO_x and CO, together with the already mentioned greenhouse gas CH₄, lead via a number of complex chemical reactions to the production of tropospheric ozone [Crutzen and Zimmermann, 1991;

Lelieveld and Van Dorland, 1995; Roelofs et al., 1997]. In the stratosphere, increases of CFCs cause a depletion of ozone. In the vicinity of the tropopause, aircraft emissions result in ozone increases [*Fortuin et al., 1995a*]. The radiative effects of tropospheric increases and stratospheric decreases of ozone are quite uncertain due to the fact that patterns of change are highly variable in space and time [*Fortuin et al., 1995b*]. Moreover, the radiative forcing is strongly dependent on the altitude at which ozone changes occur [*Lacis et al., 1990; Van Dorland and Fortuin, 1994*]. Changes in the tropospheric sulfate aerosol content exhibit even larger uncertainties in the radiative forcing. Anthropogenic sulfur emissions lead to the formation of sulfate aerosols, which act to cool the climate by virtue of their ability to scatter shortwave radiation back to space, known as the direct effect. The radiative forcing due to the indirect effects of aerosols, i.e. the changes the optical properties and lifetimes of clouds, has a very low confidence level [*IPCC, 1994; 1995*]. Due to the large uncertainties in the direct as well as indirect cooling effects of sulfate aerosols, the total radiative forcing of greenhouse gases and aerosols from human activities is poorly known, ranging from $+0.5 \text{ Wm}^{-2}$ to $+2.5 \text{ Wm}^{-2}$.

2.6.3 Climate Models

Coupled atmosphere-ocean general circulation models (GCMs) are the state-of-the-art tool for understanding the present climate and estimating the effects of natural as well as anthropogenic climate perturbations. Such comprehensive models include many physical processes and their mutual interactions. Since the required computer resources to run these models for centuries are substantial, it is not feasible to perform large amounts of climate simulations. Moreover, the computational cost puts restrictions on the model complexity and resolution. The evaluation with observational data is essential for getting at least some confidence in the present generation of climate models, although it is difficult or even impossible to get correspondence with the real world in all aspects. With respect to future projections using identical scenarios, climate models show qualitatively the same response patterns on the larger scales, although global mean near surface air temperature changes vary by a factor of three among the models [*IPCC, 1990; 1995*]. This implies a spread in equilibrium temperature response of $+1.5$ to $+4.5 \text{ K}$ for a doubling of CO_2 . On the regional scales, temperature changes and especially changes in hydrological parameters, such as precipitation, are highly uncertain.

Because on the global scale the perturbation of the radiation balance at the top of the atmosphere is the determining factor for climate change, simpler models than coupled GCMs are useful to study global average temperature change, with the advantage of consuming substantially less computer time for the same integrations. An example of such a simple model is a 1D radiative-convective model (RCM) in which the vertical structure of the atmosphere is resolved in order to perform accurate radiative transfer computations. The fast redistribution of energy in the troposphere through sensible and latent heat flows is taken into account by postulating a critical temperature gradient in the troposphere. RCMs are calibrated towards the global mean

energy balance. With these RCMs it is feasible to compute the global average equilibrium response on radiative forcing mechanisms in which various climate feedbacks can be included. If RCMs are coupled to (simple) 1D ocean models, simulations can be performed of the transient response due to radiative perturbations (see Chapter 5).

2.6.4 Uncertainties in Climate Response

Uncertainties in the response to anthropogenic changes of the composition of the atmosphere, as computed by climate models, are mainly caused by uncertainties in the radiative forcing, the climate sensitivity as well as in the partition between heat storage in the ocean and directly returned energy towards the atmosphere. As already stated in section 2.6.2, the total anthropogenic radiative forcing is estimated to be $1.5 \pm 1.0 \text{ Wm}^{-2}$. This large range is mainly caused by the uncertainties in the cooling effects of aerosols.

The coupling between radiative forcing and equilibrium temperature response is called the climate sensitivity, expressed in K/Wm^{-2} . For the present generation of 3D climate models, this climate sensitivity parameter is ranging from 0.3 to 1.1 K/Wm^{-2} (see section 2.4.2). This range by a factor of three as mentioned in section 2.6.3 is mainly the result of uncertainties in the climate feedbacks induced by temperature dependent processes in the climate system. The response to perturbations of the radiation balance can either be amplified or damped as the result of these feedback mechanisms. Most pronounced is the positive water vapor feedback: if the temperature increases, e.g. due to increases of the atmospheric CO_2 level, the air will contain more water vapor. This is based on the observation that in our present climate the relative humidity especially over the oceans is quite constant (see section 2.4.3). Since water vapor is an important greenhouse gas, increases herein result in an amplification of the global warming. The feedbacks related to changes in cloud properties are highly uncertain and are therefore largely responsible for the uncertainties in climate sensitivity [Cess *et al.*, 1995; IPCC, 1995].

The partition between the heat storage in the oceans and the directly rendered energy into the atmosphere through either longwave radiation or latent and sensible heat flows, is largely dependent on the thermal and salinity structure of the oceans, thereby regulating the heat diffusion as well as the upwelling processes. Since the climate system acts as a low pass filter due to the large heat capacity of these oceans, the partition is also dependent on the period of the climate perturbation. Moreover, it is very difficult to evaluate this partition of heat with observational data. Although the mechanisms of the human influence on the radiation balance are physically well understood, accumulation of uncertainties results in poor estimates of subsequent global mean temperature changes.

2.7 Summary and Conclusions

The science of climate change can be traced back to more than one century ago, when Svante Arrhenius made the first quantitative statements on the climate effects due to changes of CO_2

concentrations. However, in the first half of the twentieth century it was widely believed that CO₂ concentrations in combination with the water vapor amount were high enough to be saturated with respect to infrared radiation. Renewed interest came in the 1950s. Due to the rapid development of computer technology scientists were able to run climate models. At present, the science of climate change has grown into a multidisciplinary field of research.

The knowledge on radiative processes, crucial for the understanding of climate change, went through a rapid development in the beginning of the twentieth century in connection with quantumphysics. Atmospheric conditions allow simplifications of the radiative transfer equation. Firstly, solar and terrestrial radiation can be separated in radiative transfer schemes by virtue of the different temperatures of the sun and the earth-atmosphere system. Secondly, the pressure in the lowest 50 km of the atmosphere is high enough to cause local thermodynamical equilibrium, simplifying the infrared (thermal) emission by greenhouse gases to be the product of black body radiation and the absorption coefficient, which is highly selective with regard to frequency.

The energy flows of the global and annual mean climate can be derived from a combination of measurements and models. The atmosphere is heated by absorption of shortwave radiation (about 80 Wm⁻²) as well as by latent and sensible heat flows from the surface into the troposphere (about 95 Wm⁻²). In addition, the atmosphere is effectively cooled by infrared radiation (about 175 Wm⁻²), indicating that longwave emission at the atmospheric boundaries is much larger than longwave absorption in the atmosphere. Paradoxically, this cooling corresponds to a substantial natural greenhouse effect of about 33 K. Therefore, doubling the CO₂ amount also causes an enhancement of this longwave cooling. This appears to be about 3 Wm⁻² in the new equilibrium state of our (model) climate using the water vapor feedback. Uncertainties in the energy flows are at least as large as the computed present radiative perturbations due to increases of greenhouse gases. Although the uncertainties in the energy flows affect global average climate with respect to the distribution of energy over the solar, infrared and non-radiative fluxes, their impact on the enhanced greenhouse effect is limited, because radiative flux changes at the tropopause (and at the top of the atmosphere) are hardly affected by these uncertainties.

The thermal structure of the atmosphere, as a consequence of the presence of radiatively active constituents in combination with tropospheric heating by latent and sensible heat flows, is in turn important for the cascade of infrared absorption and emission as well as for the perturbations therein due to the changes of greenhouse gas concentrations. Moreover, by virtue of this thermal structure the climate system can be separated thermodynamically into a stratosphere and a tightly coupled surface-troposphere system, which possess a short and a long timescale for adjustments to radiative perturbations, respectively. The radiative forcing is therefore a measure of the subsequent surface temperature changes, which appears to be near-invariant to the nature of forcing mechanisms [Ramaswamy and Chen, 1997]. In fact, this emphasizes the dominant role of radiative transfer, a process on molecular scale, in the climate system, being a large scale phenomenon by virtue.

The link between radiative forcing and surface temperature change facilitates the determi-

nation of the relative contributions of atmospheric constituents to the natural greenhouse effect using our Radiative-Convective Model. Water vapor contributes most due its abundance and its average absorption strength per molecule. Moreover, the warming effect of water vapor is much larger than the cooling effect of clouds. The amount of water vapor is strongly coupled to atmospheric temperatures, resulting in the so-called water vapor feedback, and thus dependent on the amount of greenhouse gases in the atmosphere. Among the uniformly mixed greenhouse gases, CO₂ shows the largest effect on the global mean surface temperature. The effect of doubling the CO₂ content is much smaller than removing this gas from the atmosphere due to the well-known logarithmic relationship between CO₂ mixing ratio and radiative forcing, but large enough to cause significant climate change.

The characteristics of longwave radiative transfer and its perturbations due to greenhouse gases can be understood by using a simplified analytical model of the troposphere. This model has three parameters, namely the Planck function at the surface and at the tropopause for the upward and downward component of the infrared flux, respectively, the tropospheric lapse rate of the Planck function (decreasing with altitude), and the absorption coefficient. All parameters can be chosen in arbitrary spectral intervals in order to investigate the effects of greenhouse gases in either transparent or opaque parts of the spectrum. The validity of these approximations is illustrated by comparing the characteristics, i.e. flux changes with height and extreme values, with those as calculated by the radiative transfer scheme used in this thesis. Using a combination of the analytical expressions and radiative transfer calculations, we show that the spectrally averaged penetration depth for longwave radiation near the surface is of the order of three hundred meter. In the atmospheric window region (8-12.5 μm) and in the remaining (opaque) part of the spectrum, this penetration depth is estimated to be of the order of 9 km and 9 m, respectively.

By taking the derivative of the analytical equation for the upward radiative flux with respect to the absorption coefficient, we simulate flux changes due to the increase of greenhouse gases. Although there are many differences between the various greenhouse gases in the atmosphere due to the strength of the infrared absorption lines, their locations in the longwave spectrum and their present concentrations, increases in the concentration of greenhouse gases always lead to an increased opacity of the atmosphere. We demonstrate that the upward longwave flux is always reduced if the Planck lapse rate is positive, i.e. for a decrease of temperature with altitude, which appears to be the crucial parameter for the enhanced greenhouse effect. However, in the opaque limit these flux reductions become very small, e.g. in the center of the 15 μm band of CO₂, which is known as saturation. Furthermore, we show that for greenhouse gases, active in the window region (e.g. CFCs), this reduction of the upward flux at the tropopause, contributing to a positive radiative forcing, is caused by further attenuation of the terrestrial flux and even partly counteracted by an increase of the upward atmospheric flux. For greenhouse gases, active in the opaque parts of the spectrum, such as the most important absorption bands of CO₂, the terrestrial flux reduction is quite small at tropopause level as compared to the decrease in atmospheric flux. The downward flux from the stratosphere increases due to increases of greenhouse gases (which

cannot be shown with this tropospheric model), enhancing the positive radiative forcing due to the aforementioned upward flux reduction.

Furthermore, we express upward and downward radiative fluxes in terms of effective temperature. We show that this temperature is a measure of altitude in the troposphere at which the longwave radiation is effectively emitted. From this point of view, it can be demonstrated that step increases of greenhouse gases result in longwave radiation into space, which is emitted from a higher effective altitude. This implies a decrease in effective temperature if the emission level is situated in the troposphere, which is generally the case except for CO₂ changes in a small spectral region close to the center of the 15 μm band. Similarly, the downward longwave radiation at the earth's surface is increased and thus originates from a lower atmospheric altitude.

Although the mechanism of the enhanced greenhouse effect due to increases of greenhouse gases is well understood, we can only make poor estimates of the total human influence on climate in terms of global mean temperature changes. In the first place large uncertainties are associated with the direct and indirect cooling effects of aerosols. Secondly, the climate sensitivity parameter is not well known due to uncertainties in climate feedbacks. Thirdly, some uncertainty is associated with the partition of heat stored in the ocean and the directly returned energy towards the atmosphere in case of a disturbed radiation balance. In addition, direct proof of the human influence on climate cannot be extracted from the observed temperature record, because the amplitude of internally and externally driven natural variability of the climate system is not well known.

The items offered in this chapter are meant to provide a useful basis for the understanding of our approach to the subject of radiation and climate. Subsequently, we construct a broad band radiative transfer scheme for climate modelling purposes, evaluated with measurements of the downward longwave flux at the surface (Chapter 3). We compute the global patterns of the radiative forcing due to increases of tropospheric ozone and sulfate aerosols, being the components with the largest uncertainty (Chapter 4). And finally, we make an attempt to attribute several forcing mechanisms to the global and annual mean temperature observed since 1856 by calculating their transient temperature responses using a 1D climate model (Chapter 5).

